الـجـمـــهـوريـــة الجـزائــريـــة الديمقراطية الـشـعـــــبـية

PEOPLE'S DEMOCRATIC REPUBLIC OF ALGERIA

وزارة التعليم العالي و البحث العلمي

MINISTRY OF HIGHER EDUCATION AND SCIENTIFIC RESEARCH

جـامعة حسيبة بن بوعلي - الشلف -

Hassiba Benbouali University of Chlef (U.H.B.C)

Faculty of Technology

Electrical Engineering Department

End-of-study project thesis with a view to obtaining the degree

MASTER

Field: Sciences & Technologies

Sector: Electrotechnical

Option : Electromecanical

Theme

Techno-economic analysis of an autonomous PV/DG system using different solar monitoring and battery storage: case study chlef (El hadjadj)

Presented by:

Abderrahim **AMEUR** & Abelmalik **MERZOUG**

Graduated on 24/06/2025 before the jury composed of:

Miss. F.BELOUAZANI	MAA	UHBC	President
Mr. A.ELEZAR	MCB	UHBC	Examiner
Miss. A.TOULBIA	MCA	UHBC	Examiner
Mr. M. DEKKICHE	MCA	UHBC	Supervisor

Promotion : 2024/2025

ملخـــص

تُحلل هذه الدراسة نظام طاقة هجينًا مستقلًا عن الشبكة في الشلف (الحجاج). يجمع هذا النظام بين ألواح الطاقة الشمسية (مع أنظمة تتبع متنوعة)، ومولد ديزل، وبطاريات. تم تقييم أربع تكوينات: نظام الإمالة الثابتة، ونظام HSAT، ونظام VSAT، ونظام DAT، باستخدام تحسين MPPT. أظهرت محاكاة HOMER Pro أن نظام DAT يُنتج أعلى طاقة (37,788 كيلوواط/ساعة سنويًا). يُعد نظام الإمالة الثابتة بزاوية 38 درجة الأكثر اقتصادًا (NPC: 21,985 دولارًا أمريكيًا؛ COE: 0.0863 دولارًا أمريكيًا/كيلوواط/ساعة). تُبرز النتائج التوازن بين أداء الطاقة والتكلفة في المناطق النائية.

Abstract

This study analyzes a hybrid off-grid energy system in Chlef, (El Hadjadj). It combines PV panels (with various tracking systems), a diesel generator, and batteries. Four configurations are assessed: fixed-tilt, HSAT, VSAT, and DAT, using MPPT optimization. HOMER Pro simulations show DAT yields the most energy (37,788 kWh/year). The fixed-tilt at 38° is the most economical (NPC: \$21,985; COE: \$0.0863/kWh). Results highlight the trade-off between energy performance and cost for remote areas.

Résumé

Cette étude analyse un système énergétique hybride hors réseau à Chlef (El Hadjadj). Il combine des panneaux photovoltaïques (avec divers systèmes de suivi), un générateur diesel et des batteries. Quatre configurations sont évaluées : inclinaison fixe, HSAT, VSAT et DAT, en utilisant l'optimisation MPPT. Les simulations HOMER Pro montrent que le DAT produit le plus d'énergie (37 788 kWh/an). L'inclinaison fixe à 38° est la plus économique (NPC : 21 985 $; COE : 0,0863 $/kWh). Les résultats mettent en évidence le compromis entre performance énergétique et coût pour les zones reculées.

Dedication

We dedicate this thesis to those who supported and encouraged us to carry out this research, as well as to those who care deeply about our success.

Thanks

First, we thank Allah, the Almighty, who granted us the will, patience, and courage necessary to complete this modest project.

We would like to express our deep gratitude to our supervisor, Dr. Mohamed DEKKICHE, Assistant Professor at the University of Chlef, for his insightful advice, constant support, availability, and encouragement throughout the completion of this dissertation.

We also extend our sincere thanks to all the faculty members of the Department of Electrical Engineering at the Faculty of Technology at the University of Chlef for the quality of their teaching, their guidance, and their support.

Our deepest thanks also go to our parents and families for their unconditional support, their sacrifices, and their faith in us. Without them, we probably would not have reached this stage.

Finally, we warmly thank all those who, directly or indirectly, contributed to the completion of this work.

Nomenclature

Greek symbols

α_P	Temperature power coefficient (%/°C)
β_T	Coefficient of variation of yield
$\eta(t)$	System yield (%)
η_{PV}	PV yield (%)
$\eta_{ref\ m}$	PV module reference yield (%)
η_{inv}	Inverter yield (%)
η_m	Yield of the modules (%)
σ	Hourly self-discharge rate
η_{inv}	Inverter yield (%)
τ_{inv}	Inverter load rate

Latin symbols

F_p	System losses factor
$T_{ref\ c}$	Cell reference temperature (°C)
T_c	Cell temperature (°C)
P_{PV}	PV power (W)
T_a	Ambient temperature (°C)
G_{inc}	Incident hourly radiation (kWh/m^2/j)
A_{PV}	Total catchment area (m^2)
$I_{DG,max}$	Maximum current of DG (A)
NPC	Net present cost ($)
COE	Cost of energy ($/kWh)
CRF	Capital recovery factor
i	Real annual interest rate (%)
C_{bat}	Battery storage capacity (Wh/Ah)
X_{DG}	DG charge rate (%)
E_{bat}	Energy of the battery (Wh)
E_S	Energy produced by the source (Wh/Ah)

E_L	Energy required by the load (Wh/Ah)
P_{losses}	Electrical losses (%)
E_{tot}	Total enegy (kWh/y)
$C_{ann,\ tot}$	Total annual cost of the system ($/y)
P_{inv}	Nominal power of the inverter (%)
$P_{O,inv}$	Inverter output power (kW)
N	Projet lifetime (y)
I	Annual interest rate (%)
$P_{I,inv}$	Inverter input power (kW)
N_p	Number of branches in parallel
N_S	Number of modules in series
$I_{PV,max}$	Maximum input current (A)
P_{MPPT}	MPPT converter nominal power (kW)
$P_{PV,max}$	PV maximum power (kW)
G_T	Solar radiation incident on the panels (kW/m^2)
$G_{T,NOCT}$	Solar radiation at which NOCT is defined (0.8 kW/m^2)
$I_{sc,m}$	Short-circuit current of the module (A)
$U_{oc,m,\ max}$	Maximum open-circuit voltage of the module (V)
q_{DG}	Fuel consumption of diesel generators (L/h)
P_{DG}	DG Power (W)
P_{DG},nom	DG Nominal Power (W)
U_{PV},max	Maximum input voltage (V)

Abbreviation

HES	Hybride energy system
V	Volts
W	Watt
m	Metter
y	Year
A	Ampere
SOC	State of Charge
DG	Diesel generator
AC	Alternating current

DC	Direct current
PV	Photovoltaic
MPPT	Maximum Power Point Tracker
NOCT	Nominal Operating Cell Temperature
HOMER	Hybrid Optimization Model for Electric Renewables
HSAT	Horizontal Single-Axis Tracking
DAT	Dual Axis Tracker
FTS	Fixed-Tilt System
VSAT	Vertical Single Axis Tracking

Index

Ann	Annual
I	Input
J	Joule
nom	Nominal
ref	Reference
tot	Total
o	Output
bat	Battery
inv	Inverter
m	Module
sc	Short-circuit
oc	Open-circuit
c	Cell
a	Ambient

List of figures

Chapter I

Figure I.1. Non-renewable energy resources. 16

Figure I.2. Gas-fired power plants. 17

Figure I.3. Coal fired power plants. 17

Figure I.4. Oil-fired thermal power station. 18

Figure I.5. Nuclear power plant. 18

Figure I.6. Different renewable energies. 19

Figure I.7. Solar Photovoltaic and Solar thermal panels. 19

Figure I.8. Biomass power plants. 20

Figure I.9. Geothermal power plants and their use for electricity production. 20

Figure I.10. Hydroelectric Plant. 21

Figure I.11. Wind field Generation and Transmission System. 21

Figure I.12. Conventional energy vs renewable energy. 22

Chapter II

Figure II.1. Annual global sunshine in the world kWh/m^2/y. 24

Figure II.2. Explain the principle of conversion in PV systems. 25

Figure II.3. Composantes d'un champ de modules photovoltaïques. 27

Figure II.4. Identical cells in series. 27

Figure II.5. Identical cells in parallel. 27

Figure.II.6. (a) Typical solar panel architecture with protective diodes (b) Failure of one of the cells in the PV module and activation of the bypass diode. 28

Chapter III

Figure III 1. Autonomous PV/DG system using battery storage. 31

Figure III 2. Functional analysis of a PV. 32

Figure III 3. Functional analysis of a DG. 33

Figure III 4. Diesel group. 33

Figure III 5. Functional analysis of a battery. 34

Figure III 6. Functional analysis of a converter. 35

Figure III 7. Block diagram of MPPT controller. 37

Chapte IV

Figure IV 1. Flowchart describing the optimization and modeling stages for the design of the HES. 40
Figure IV 2. Geographical location of the study the house (El Hadjadj, Chlef). 41
Figure IV 3. Represents the monthly temperature of the site. 42
Figure IV 4. The variation of average solar irradiation. 42
Figure IV 5. Electrical load. 43
Figure IV 6. PV tracking systems (a) Fixed-facing at four different tilt angles (b) Horizontal single-axis solar tracker (c) Vertical single-axis solar tracker (d) Dual axis tracker 46
Figure IV 7. Energy production and excess of one year for different PV tracking techniques. 47
Figure IV.8. PV penetration of one year for different PV tracking techniques. 47
Figure IV 9. Capacity factor for different PV tracking techniques. 48
Figure IV 10. Daily power comparison between PV and MPPT converter. 49
Figure IV 11. Monthly generation of the PV/DG system. 49
Figure IV 12. Cost breakdown of various components of FTS/38°hybrid system. 50
Figure IV 13. Cash flow of the optimum system listed by (a) component, (b) cost type. 52
Figure IV 14. PV power output throughout the year for the FTS/38° system. 52
Figure IV 15. DG power output throughout the year for the FTS/38° system. 53
Figure IV 16. State of charge over one year. 53
Figure IV 17. System FTS/38° of converter. 54
Figure IV 18. Instantaneous renewable output divided throughout the year for the FTS/38° by load. 54
Figure IV 19. NPC for FTS/38° and grid extension as function of distance. 55

List of tables

Table II.1: Sunshine received in Algeria by climatic region. 24
Table II.2: Performance of the different cell technologies. 25
Table IV 1: PV parameters. 44
Table IV 2: DG parameters. 44
Table IV 3: Converter parameter 44
Table IV 4: Battery parameters. 45
Table IV 5: MPPT parameter. 45
Table IV 6: Tracking systems cost. 46
Table IV 7: Results for HES. 50

SUMMARY

ملخص – Abstract…… 1
Dedication…… 2
Thanks…… 3
Nomenclature…… 4
List of figures…… 7
List of tables…… 9
Table of contents…… 10
General introduction…… 13

CHAPTER I: **General information on the different energy sources**

I.1. Introduction…… 16
I.2. Non-renewable energy sources…… 16
I.3. Different types of non-renewable energy plants…… 16
I.3.1. Gas-fired power plants…… 16
I.3.2. Coal fired power plants…… 17
I.3.3. Oil-fired thermal power station…… 17
I.3.4. Nuclear power plants (petroleum)…… 18
I.4. Renewable energy sources…… 18
I.5. Different types of renewable energy plants or field…… 19
I.5.1. Solar energy…… 19
I.5.2. Biomass power plants…… 20
I.5.3. Geothermal power plants…… 20
I.5.4. Hydroelectric plant…… 20
I.5.5. Wind field…… 21
I.6. Compare between renewable and non-renewable energies…… 21
I.7. Conclusion…… 22

CHAPTER II: **Photovoltaic solar energy**

II.1. Introduction…… 24
II.2. Solar deposit in the world…… 24
II.2.1. Solar potential in Algeria…… 24

II.3. Photovoltaic conversion principle.......... 25
II.3.1. Types of solar panels.......... 25
II.4. Photovoltaic generator.......... 26
II.4.1. Protection of the PV generator.......... 28
II.5. Advantages and disadvantages of solar PV.......... 28
II.6. Conclusion.......... 29

CHAPTER III: **Sizing of the HES**

III.1. Introduction.......... 31
III.2. Architecture of an autonomous hybrid PV/DG system with battery storage.......... 31
III.3. Technical sizing.......... 31
III.4. Sizing a PV.......... 31
III.4.1. Functional analysis of a PV.......... 32
III.5. Sizing of a DG.......... 33
III.5.1. Functional analysis of a DG.......... 33
III.6. Storage system sizing.......... 34
III.6.1. Functional analysis of a battery.......... 34
III.6.2. Battery charging model.......... 34
III.6.3. Battery discharge model.......... 35
III.7. Sizing of the conversion system (converter).......... 35
III.7.1. Functional analysis of the bidirectional converter.......... 35
III.8. Sizing of the MPPT converter.......... 37
III.8.1. MPPT converter.......... 37
III.9. Conclusion.......... 38

CHAPTER IV: **Results and analysis**

IV.1. Introduction.......... 40
IV.2. HES modeling and optimization flowchart.......... 40
IV.3. Presentation of the HOMER pro software.......... 41
IV.4. Dimensioning by HOMER pro software.......... 41
IV.4.1. Geographical location.......... 41
IV.4.2. Climate data.......... 41
IV.4.3. Irradiance of the study site.......... 42
IV.4.4. Load Profile.......... 43
IV.5. Technical - economical parameter of components for our study.......... 43

IV.6. Results and discussion… 46
IV.6.1. Technical comparison between different tracking systems… 46
IV.6.1.1. Energy production and excess… 46
IV.6.1.2. PV penetration… 47
IV.6.1.3. Capacity factor… 47
IV.6.1.4. Impact of MPPT on Performance… 48
IV.6.1.5. Monthly generation… 49
IV.6.2. Economic analysis 50
IV.6.2.1. Cash flow by component and cost type 51
IV.7. Operation status of the Optimal PV tracking technique (FTS/38°) 52
IV.7.1. PV electrical summary 52
IV.7.2. DG electrical summary 53
IV.7.3. Battery storage 53
IV.7.4. Converter electrical summary 54
IV.7.5. Renewable penetration 54
IV.8. Grid extension electrification cost 55
IV.9. Conclusion 55

General conclusion 56
Bibliographic references 58

General introduction

General introduction

As part of the global energy transition, researchers are focusing on energy systems suited for rural areas lacking reliable grid access. Hybrid energy systems (HES), which combine photovoltaic (PV) panels, diesel generators (DG), and battery storage, are a promising solution. This study is divided into four chapters that build the foundation for designing autonomous HES. The theoretical chapter explains the need for hybridization and energy reliability. The technological section describes system components, including PV tracking types, batteries, and DGs. The methodological chapter focuses on modeling and optimization, using tools like HOMER Pro. Finally, the practical application evaluates system performance in a real case in Chlef, Algeria. Together, these chapters demonstrate how HES can balance sustainability, reliability, and cost. They support the deployment of clean energy in remote regions.

Chapter I compares and contrasts renewable and non-renewable energy sources in this summary of the various energy sources. It draws attention to the sustainability challenges of fossil fuels while drawing attention to the positive effects of renewable resources from the standpoint of sustainable development.

Chapter II points out solar energy from photovoltaics. In addition to highlighting Algeria's abundant solar potential, it explains the photovoltaic conversion principle, solar panel types. Advantages and disadvantages of solar PV.

Chapter III discusses the hybrid PV/DG system with storage's technical sizing. In order to guarantee the best possible balance between energy production and storage, it describes the calculations and models used to size each component, including PV, DG, batteries, converters, and MPPT.

Finally, Chapter IV applies the developed knowledge through simulations using HOMER Pro. This allows for the analysis of different technical and economic configurations of the HES. The simulation helps evaluate performance, cost, and energy reliability. Its purpose is to identify the most efficient and sustainable system design. The case study focuses on providing reliable power to a rural area in Algeria.

Chapter I

General information on the different energy sources

I.1. Introduction

In general, there are two categories of energy sources: renewable and non-renewable. Non-renewable resources, like coal and oil, are limited and harmful to the environment, and renewables begin from natural, replenishable processes like sunlight and wind. The availability, long-term sustainability, and environmental impact of both categories are compared in this chapter.

I.2. Non-renewable energy sources

Conventional energy includes resources such as natural gas, carbon, petroleum, nuclear (figure I.1).

Figure I.1. Non-renewable energy resources [1].

I.3. Different types of non-renewable energy plants

I.3.1. Gas-fired power plants

They are a type of fossil fuel power station that uses the chemical energy stored in natural gas, mostly methane, to create thermal, mechanical, and electrical energy. They do this by burning natural gas to heat water and create steam, which in turn powers turbines to generate electricity (figure I.2).

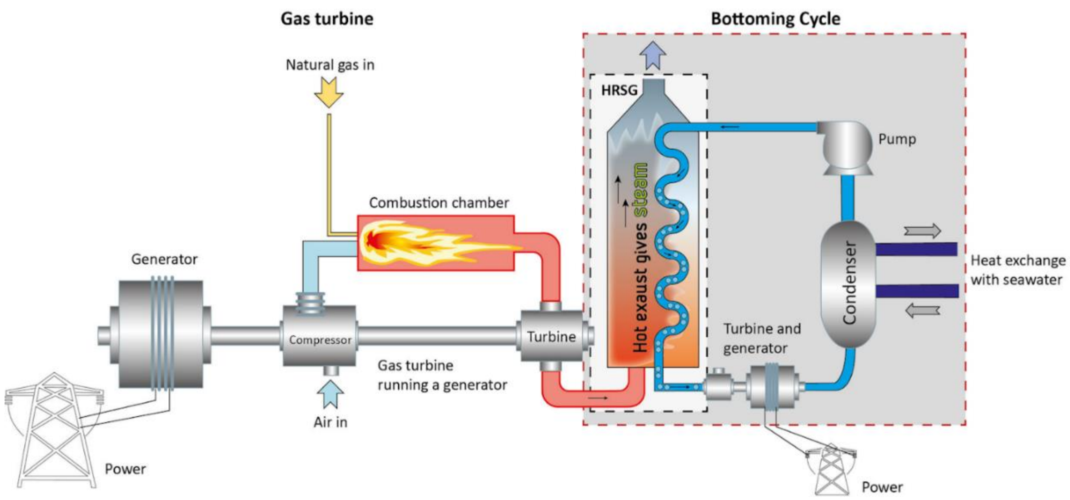

Figure I.2. Gas-fired power plants [2].

I.3.2. Coal fired power plants

Coal is burned in coal-fired power plants to generate steam and heat water, which then generates electricity. A turbine connected with a generator is powered by the steam. Thermal energy is transformed into electrical energy by this mechanical process, as shawn in the figure I.3. It is a widely used technique for producing electricity in several countries.

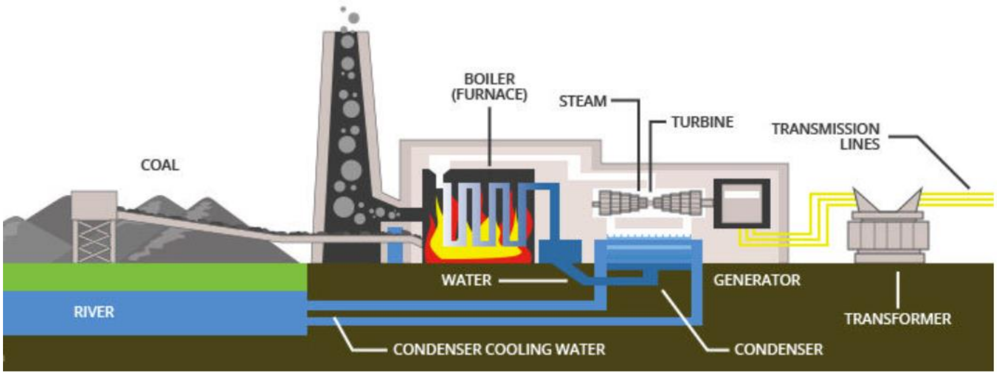

Figure I.3. Coal fired power plants [3].

I.3.3. Oil-fired thermal power station

They burn oil to create heat in order to produce electricity. According to figure I.4, this heat turns water into steam, which powers a turbine that is attached to a generator. Electrical energy is produced from the turbine's mechanical energy. It functions similarly to other thermal power plants.

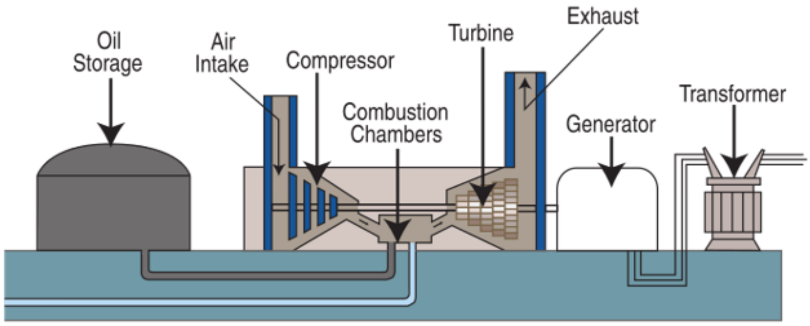

Figure I.4. Oil-fired thermal power station [4].

I.3.4. Nuclear power plants (petroleum)

They use the heat from nuclear fission to create electricity. This process releases a lot of heat as uranium atoms split in a reactor. As seen in figure I.5, the heat is converted into steam, which powers turbines that are connected to generators. A steady and continuously supply of electricity is provided by this method.

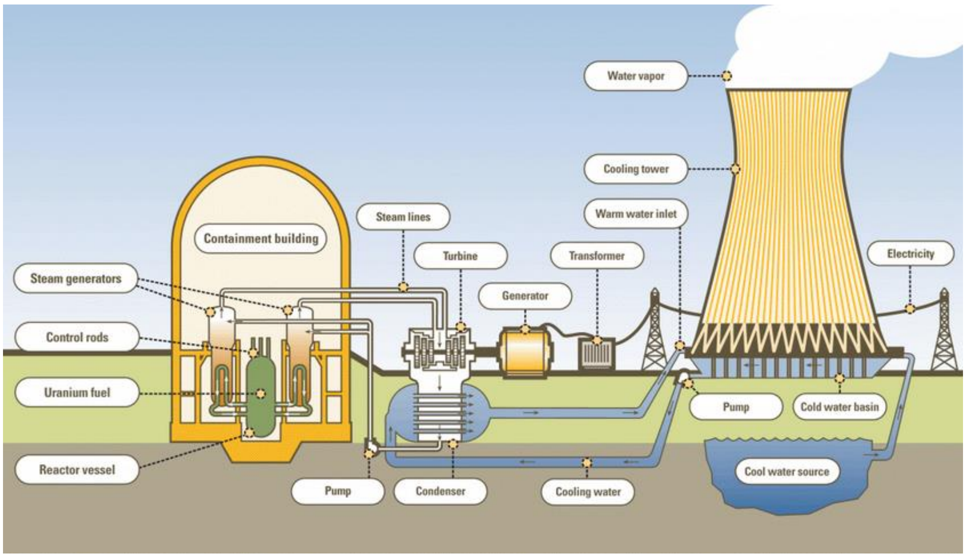

Figure I.5. Nuclear power plant [5].

I.4. Renewable energy sources

Renewable energy consists of different primary categories, each representing distinct technological approaches to sustainable power generation, these fundamental categories include in following figure I.6.

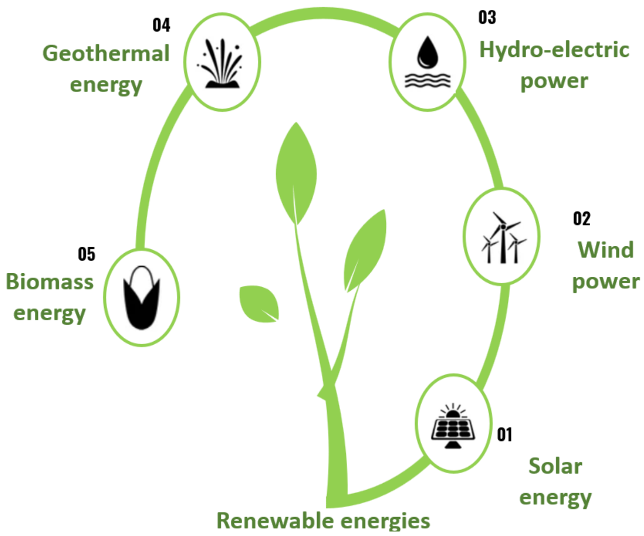

Figure I.6. Different renewable energies.

I.5. Different types of renewable energy plants or field

I.5.1. Solar energy

There are several ways to generate and use solar energy, including photovoltaic and thermal solar energy (figure I.7).

- Solar thermal energy: which simply consists of producing heat through dark panels. You can also produce with steam from the heat of the sun and then convert the steam into electricity.
- Photovoltaic solar energy: which consists of producing electricity directly from light using solar panels. This form of energy is already being exploited in many countries, especially in countries or regions without conventional energy resources such as hydrocarbons or coal [6].

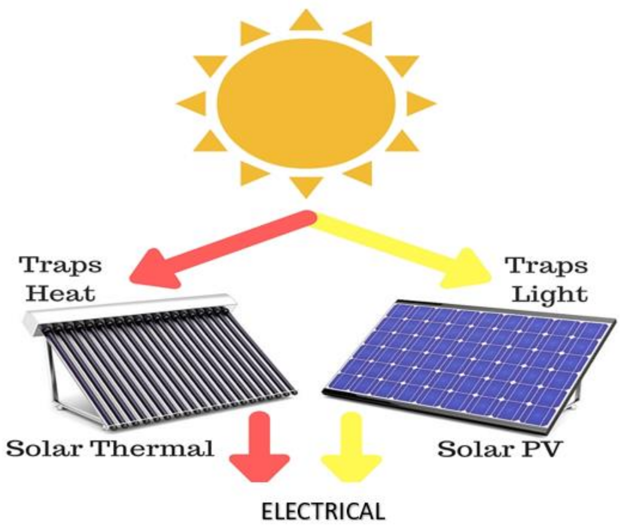

Figure I.7. Solar Photovoltaic and Solar thermal panels [7].

I.5.2. Biomass power plants

Heat is produced by burning biomass, such as wood, household waste, or agricultural waste, in order to create electricity. Biomass is a renewable energy source because it is constantly being replenished. Usually, it is burned to create steam, which powers a turbine that is attached to a generator to create electricity (figure I.8).

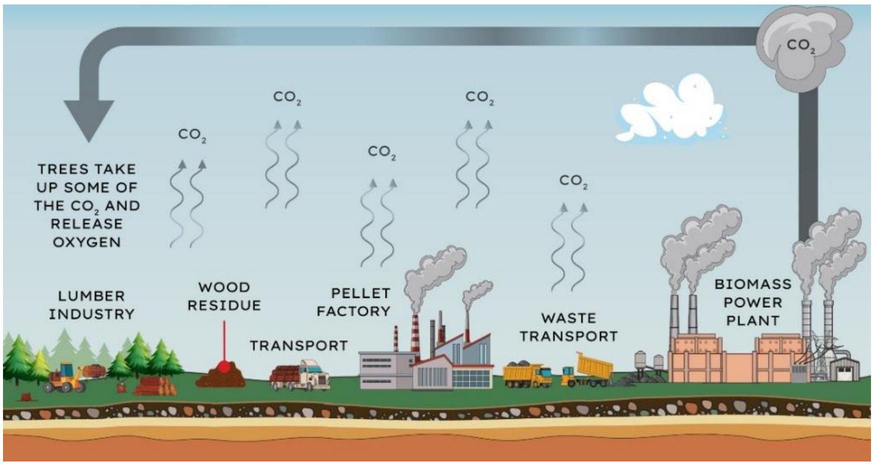

Figure I.8. Biomass power plants [8].

I.5.3. Geothermal power plants

Geothermal power plants are a renewable energy source because they use heat from the Earth's interior to create electricity. They draw steam or hot water from subterranean reservoirs to power turbines that are attached to generators. Each of the three primary varieties—dry steam, flash steam, and binary cycle—uses geothermal energy in a unique way (figure I.9).

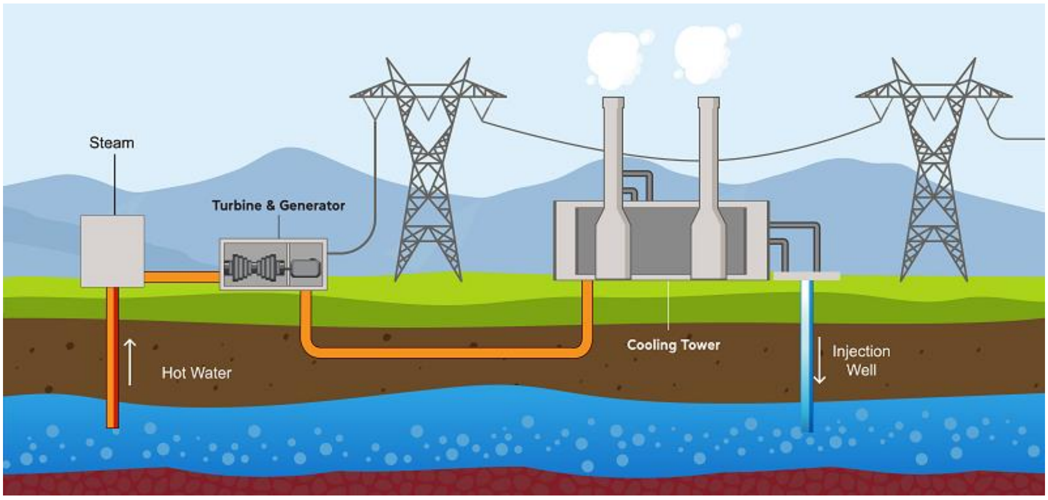

Figure I.9. Geothermal power plants and their use for electricity production [9].

I.5.5. Hydroelectric plant

Electricity is generated by using the kinetic energy of moving water. Usually, these plants are constructed close to rivers or other sources of water where the force of water movement can be used. They use a resource that is naturally replenished, making them a renewable energy source (Figure I.10).

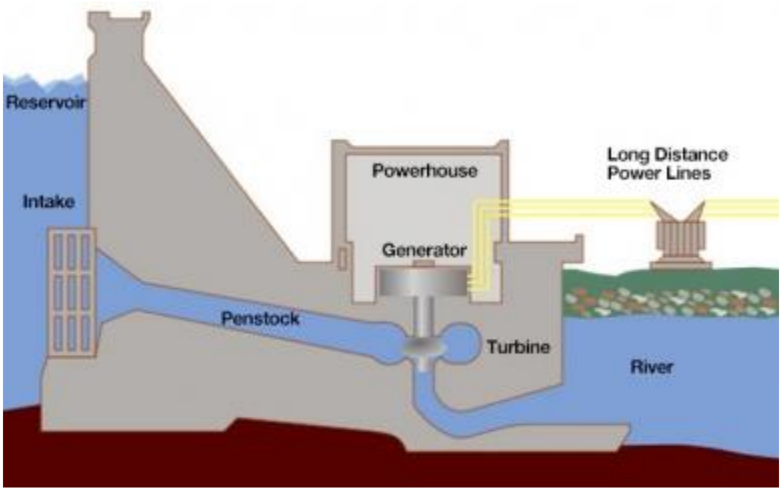

Figure I.10. Hydroelectric Plant [10].

I.5.6. Wind field

A wind turbine is a machine that transforms the kinetic energy of the wind into mechanical energy, which in turn is converted into electricity (figure I.11).

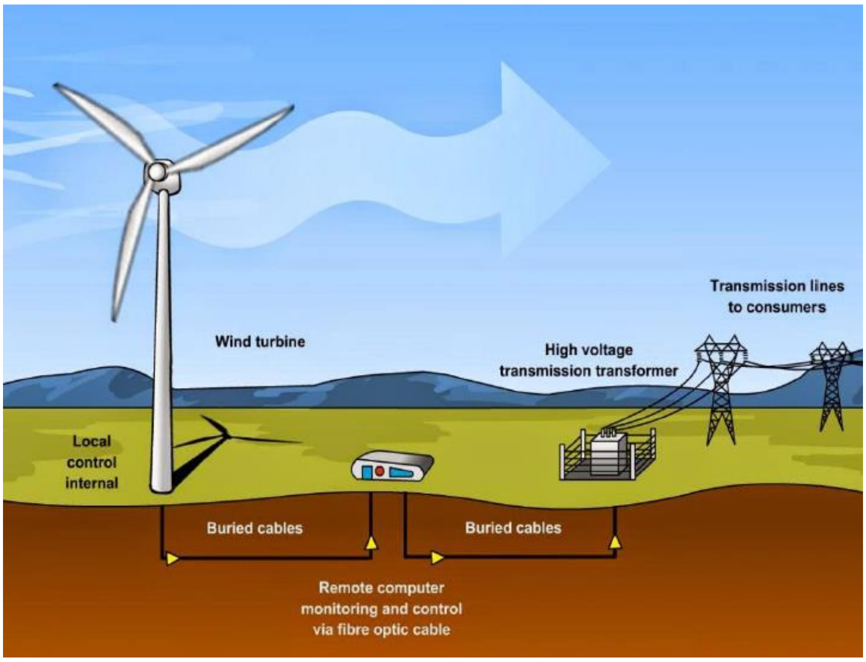

Figure I.11. Wind field Generation and Transmission System [11].

I.6. Compare between renewable and non-renewable energies

The difference lies in the nature of the renewal process and its impact on the environment. Because they are limited and only last for a short time, non-renewable energy sources like coal, natural gas, and gasoline have a harmful impact on the environment and create pollution (figure I.12).

Figure I.12. Conventional energy vs renewable energy [12].

I.7. Conclusion

The comparison demonstrates that while non-renewable sources are still widely used today, they significantly increase pollution and depletion. In the long term, renewable energies are cleaner and more sustainable. Renewables present viable and promising alternatives, even with limitations. Adopting them is crucial to creating a safe and sustainable energy future.

Chapter II

Photovoltaic solar energy

II.1. Introduction

This chapter highlights Algeria's abundant solar resources while examining the potential for solar energy both domestically and internationally. It explains the fundamentals of photovoltaic conversion as well as the primary varieties of solar panels and trackers. To emphasize their usefulness, the benefits and drawbacks of solar PV technologies are also covered.

II.2. Solar deposit in the world

Assessing a site's solar potential is key to properly sizing a solar system. Based on irradiation data from weather stations, it helps simulate system performance according to energy needs [13]. Algeria, like other southern Mediterranean countries, enjoys exceptional solar resources (figure II.1).

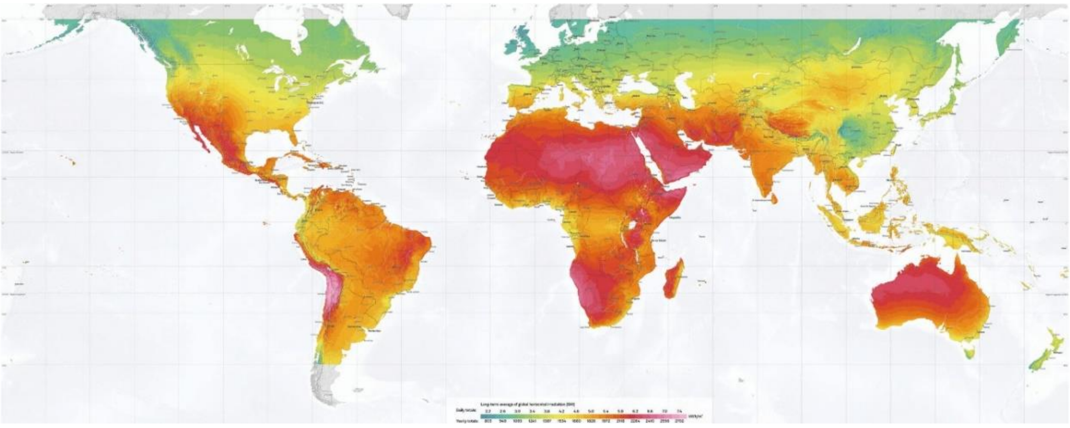

Figure II.1. Annual global sunshine in the world kWh/m^2/y [13].

II.2.1. Solar potential in Algeria

Algeria holds one of the world's richest solar resources, with annual radiation ranging from 1.700 to 2.263 kWh/m², mainly in the Sahara, which covers over 80% of its area. These significant potential positions the country favorably for large-scale photovoltaic development and clean energy production for local use or export.

Table II.1: Sunshine received in Algeria by climatic region [14].

Region	Coastal region	Highlands	Sahara
Area (%)	4	10	86
Average duration of sunshine (h/y)	2650	3000	3500
Average energy received ($kWh/m^2/y$)	1700	1900	2650

II.3. Photovoltaic conversion principle

The photovoltaic cell works thanks to the photovoltaic effect, which produces an electromotive force under the action of light. The generated voltage generally varies between 0.3 and 0.7 V depending on the material, structure and ambient temperature (figure II.2).

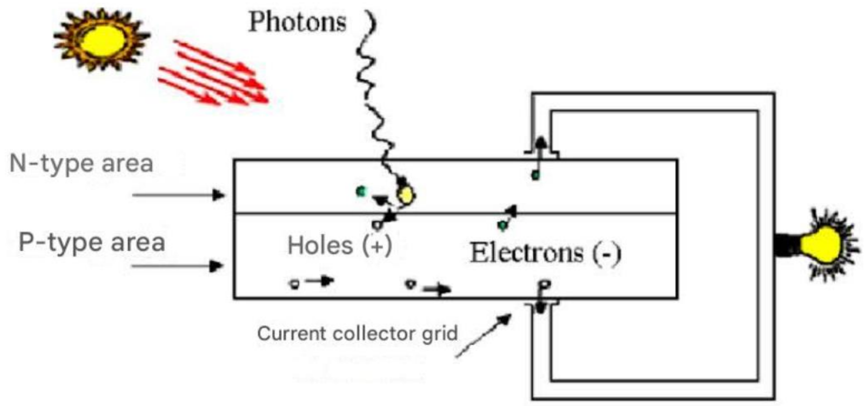

Figure II.2. Explain the principle of conversion in PV systems [15].

II.3.1. Types of solar panels

The table below shows some characteristics of solar cell types.

Table II.2: Performance of the different cell technologies [16].

Technology	Performance (%)	Lifetime (year)	Advantage	disadvantages
Monocrystalline Silicon 	14-17	35	Good performance for a cell	Student costs, loss of raw material during manufacturing

Polycrystalline silicon 	12-15	35	Good performance for a cell	Student costs, loss of raw material during manufacturing
Amorphous silicon 	6-10	<10	Eas to manufacture	Poor performance
CdTe 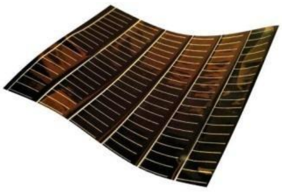	8-11	Does not assess	Absorbs 80 of the incident photons	Highly polluting cadmium
Organic cell 	10	currently low	Performance still too much	Low cost manufacturing, flexible

Monocrystalline and polycrystalline cells are the most commonly used technologies in the photovoltaic field, accounting for approximately 60% of global production.

II.4. Photovoltaic generator

A photovoltaic cell generates electrical energy through the photovoltaic effect, but its limited power when used alone limits its application. To achieve higher power, multiple cells are arranged in series and parallel. This creates a photovoltaic module designed for large-scale applications (figure II.3).

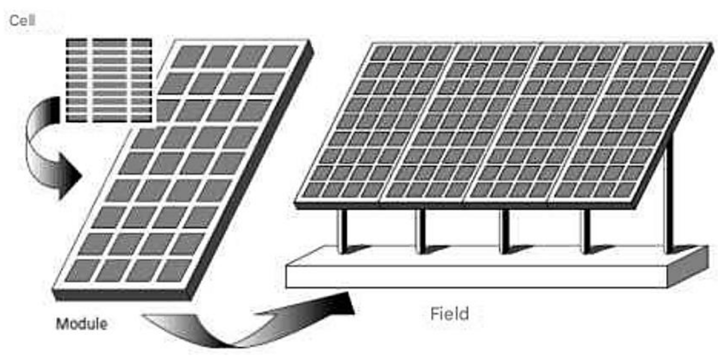

Figure II.3. Composantes d’un champ de modules photovoltaïques [17].

- Serial association

By adding identical cells in series, the current remains the same but the voltage increases proportionally to the number of serial components (figure II.4).

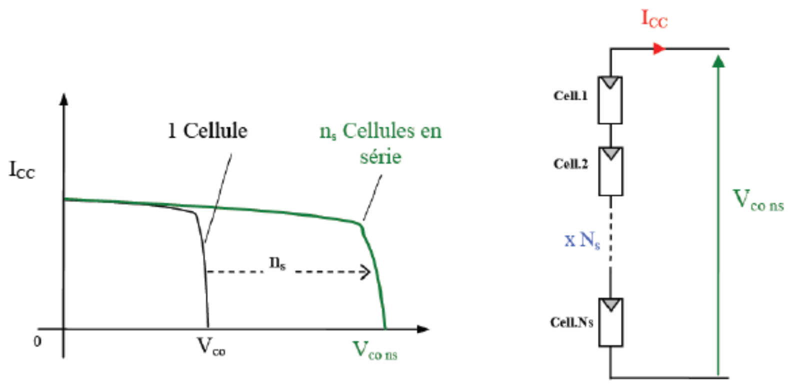

Figure II.4. Identical cells in series [18].

- Parallel association

By adding identical cells in parallel, the current remains constant but the voltage increases proportionally to the number of components put in parallel (figure II.5).

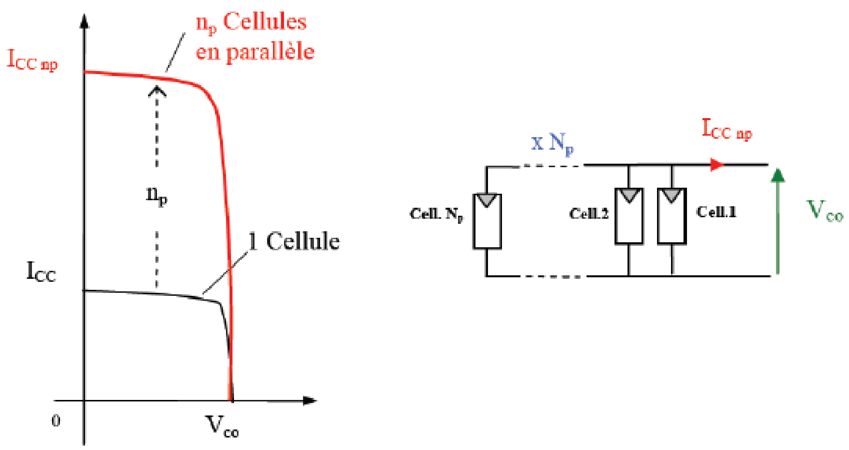

Figure II.5. Identical cells in parallel [18].

II.4.1. Protection of the PV generator

The series protection diode is used to stop parallel cell branches from being powered by series cell branches. A bypass diode is connected in parallel to lower the possibility of an excessive reverse voltage in the event of masking. The cells are shielded from reverse overvoltages by these devices (figure II.6).

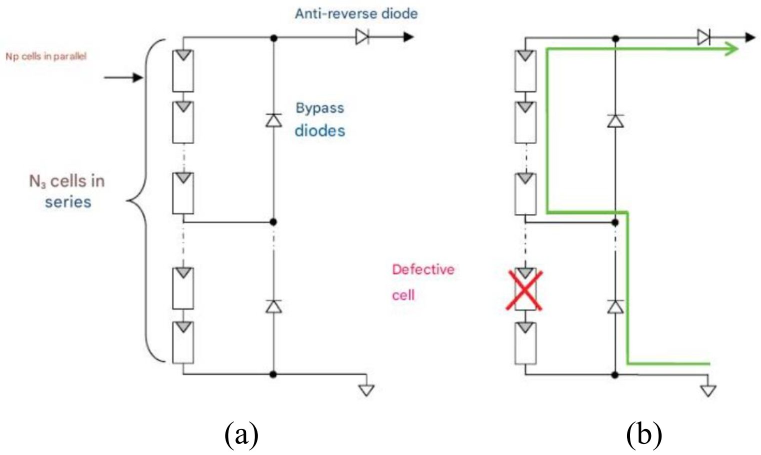

Figure II.6. (a) Typical solar panel architecture with protective diodes (b) Failure of one of the cells in the PV module and activation of the bypass diode [19].

II.5. Advantages and disadvantages of solar PV

The use of photovoltaic solar energy requires evaluating its advantages and limitations based on the constraints and needs specific to each project.

Advantages

- ✓ Sustainable and free;
- ✓ Long life (25-30 years);
- ✓ Clean, silent technology;
- ✓ Low maintenance;
- ✓ Ideal for isolated areas;
- ✓ Architectural integration possible and aesthetic;
- ✓ Rapid energy returns due to technological progress.

Disadvantages

- ✓ Production variable according to the sunshine;
- ✓ Significant initial investment despite lower costs;
- ✓ Frequent need for battery storage;
- ✓ Limited cell efficiency (20-22%);

- ✓ Need for large areas.

II.6. Conclusion

Photovoltaic solar energy is a promising solution for clean electricity generation, especially for a country like Algeria with exceptional solar potential, and with technological advances such as solar tracking systems that optimize energy capture, these systems become even more effective when integrated into Hybrid Energy Systems (HES), which will be discussed in the next chapter.

Chapter III

Sizing of the HES

III.1. Introduction

This chapter deals with the sizing of PV/DG hybrid systems, essential for a reliable energy supply in isolated areas. It presents the analysis of the main system components (PV, DG, batteries, converters and MPPT) to ensure an optimal balance between production, storage and consumption, while aiming for optimal technical performance.

III.2. Architecture of an autonomous hybrid PV/DG system with battery storage

To provide trusted power in isolated locations, the self-sufficient PV/DG hybrid system integrates solar panels, a diesel generator, and battery storage. While the battery stores excess electricity for later use, solar tracking improves energy production. Sustainable and effective energy management is ensured by an MPPT controller and an inverter (Figure III.1).

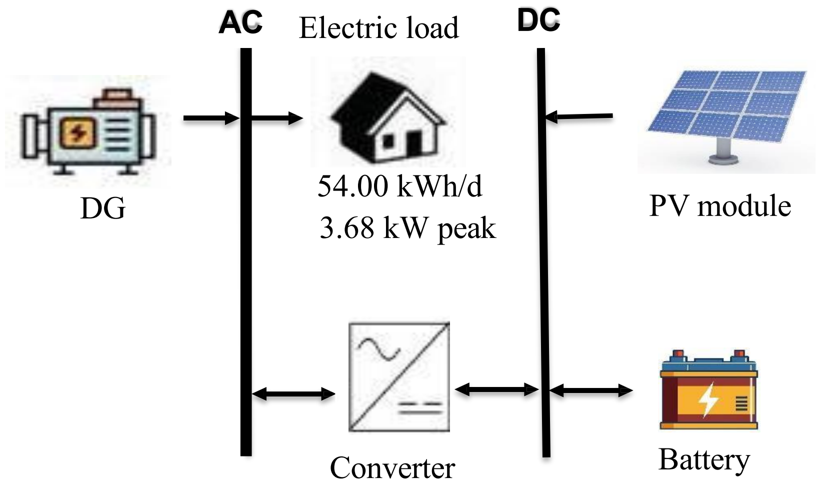

Figure III.1. Autonomous PV/DG system using battery storage.

III.3. Technical sizing

Analyzing and comparing the different possible combinations of energy sources in HES requires the use of sizing models.

The approach for sizing the hybrid system is as follows:

- Sizing a PV ;
- Sizing the DG system;
- Sizing of the battery;
- Sizing the bidirectional converter system (Inverter/Rectifier);
- Sizing of the MPPT converter.

III.4. Sizing a PV

III.4.1. Functional analysis of a PV

The main source of discontinuous energy to operate a photovoltaic panel is radiation. It converts solar energy into electricity (figure.III.2).

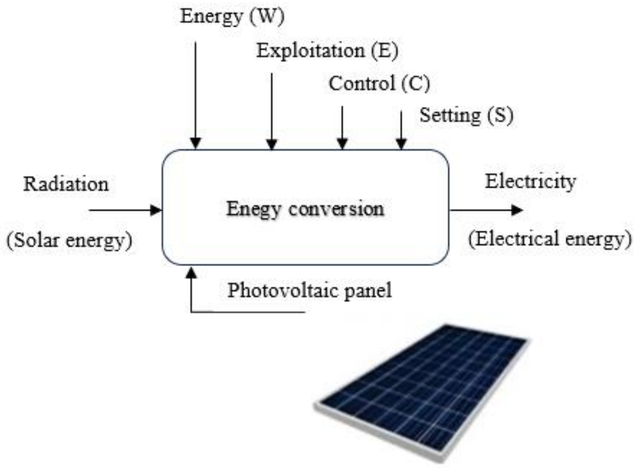

Figure III.2. Functional analysis of a PV.

The modeling of a PV aims to determine its power P_{PV} (W) and its yield η_{PV} (%), taking into account factors such as illumination and temperature which influence its performance.

When receiving an incident hourly illumination G_t (W/m^2), the PV solar generator delivers an hourly power with a total capture surface A_{pv} (m^2), is given by [20]:

$$P_{PV}(t) = \eta(t) . A_{PV} . G_{inc}(t) \quad \text{(III.1)}$$

With the system yield η(t) is given by [21] :

$$\eta(t) = \eta_m(t) . \eta_{inv} . F_P \quad \text{(III.2)}$$

And the yield of the modules ηm (t), given by :

$$\eta_m(t) = \eta_{Ref.m} . [1 - \beta_T . (T_c(t) - T_{Ref.c})] \quad \text{(III.3)}$$

Or:

$\eta_{ref\ m}$= PV module reference yield [%];

η_{inv}= Inverter yield [%];

F_p= System losses factor (connection losses, temperature losses, etc.);

β_T= Coefficient of variation of yield ;

$T_{ref\ c}$= Cell reference temperature [°];

T_c= Cell temperature [°].

The temperature T_c is calculated according to Duffie and Beckman [22]:

$$T_c(t) = T_a(t) + \left(\frac{T_{NOCT} - T_{a,NOCT}}{G_{T,NOCT}}\right) . G_{inc}(t) \quad \text{(III.4)}$$

With T_a (t), which expresses the hourly ambient temperature and T_{NOCT} (°C) represents the temperature of the cells under the conditions NOCT (Normal Operating Cell Temperature: $G_{T, NOCT}$= 0.8 kW/m^2, $T_{a, NOCT}$=20°C, Specter AM=1.5).

III.5. Sizing of a DG

III.5.1. Functional analysis of a DG

A generator set is used to connect a heat engine to a generator to produce electricity (figure.III.3).

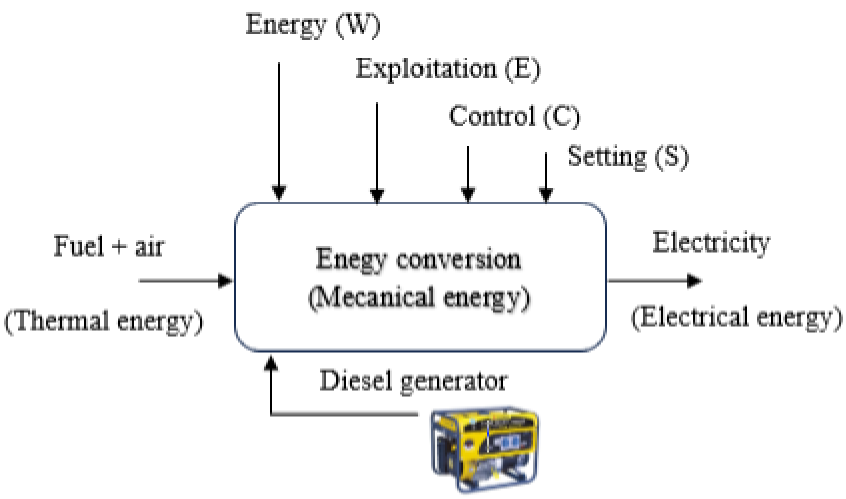

Figure III.3. Functional analysis of a DG.

The 1 kW GMI diesel generator is a compact, fuel-efficient power source ideal for remote areas and backup use, offering reliable off-grid electricity (figure.III.4).

Figure III.4. Diesel generator [23].

Power is the most important criterion when choosing a generator. We are talking about the electrical output power, not the power of the combustion engine.

The current supplied by a DG at a time (t) is given by [24]:

$$I_{DG}(t) = I_{DG,max} \cdot X_{DG}(t) \quad \text{(III.5)}$$

Or:

$I_{DG,max}$= Maximum current of the diesel generator [A];

$X_{DG}(t)$= Load rate (in % of its nominal power) at a time (t).

A diesel generator is characterized by its fuel consumption (hourly or specific). The hourly consumption of a diesel generator q_{DG} (t) is given by the following formula [25]:

$$q_{DG}(t) = a.P_{DG}(t) + b.P_{DG,nom}(t) \quad \text{(III.6)}$$

Or:

a (l/kWh) and b (l/kWh) are constants. P_{DG} (t) et $P_{DG,nom}$: Respectively the power delivered at a time t and the nominal power of the diesel generator. Their expressions are:

$$P_{DG}(t) = \sqrt{3}\,.I_{DG}(t) + U_{DG,nom\,AC}.Cos\,\varphi \quad \text{(III.7)}$$

$$P_{DG,nom} = \sqrt{3}\,.I_{DG,max}(t) + U_{DG,nom\,AC}.Cos\,\varphi \quad \text{(III.8)}$$

Or: $U_{DG,nom\,AC}$ and cos(phi) are the rated AC voltage of the diesel generator and the power factor respectively.

III.6. Storage system sizing

III.6.1. Functional analysis of a battery

A battery is a device that stores chemical energy (figure.III.5). When the battery is in operation, this chemical energy releases electricity.

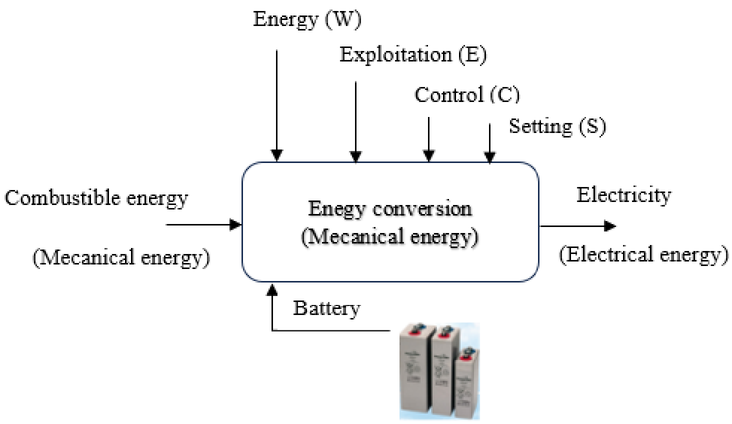

Figure III.5. Functional analysis of a battery.

Although the system can operate without batteries, their role is crucial to optimizing operations, reducing diesel use, and limiting emissions. Excess renewable energy is thus stored in the batteries.

III.6.2. Battery charging model

State of charge (SOC) is a measure of a battery's remaining energy as a percentage of its stated capacity [26]:

$$E_{bat}(t) = SOC = \frac{C_{bat}}{C_{bat\,max}} = E_{bat}(t-1)(t-\sigma) + (E_s(t) - \frac{E_L(t)}{\eta_{inv}})\,\eta_{bat} \quad \text{(III.9)}$$

E_{bat} (t)= SOC (State of Charge) = Energy stored in the battery at t, [Wh] or [Ah];

E_{bat} (t-1) = Energy stored in the battery at the initial time (t-1), [Wh] or [Ah];

σ = Hourly self-discharge rate;

E_S (t) = Energy produced by the source, [Wh];

E_L (t) = Energy required by the load at a time t, [Wh];

η_{inv} = Inverter yield.

With: $$0 \leq SOC \leq 1 \quad \text{(III.10)}$$

III.6.3. Battery discharge model

The battery discharges when consumption exceeds photovoltaic production, thus compensating for the energy deficit. [27, 28]:

$$E_{bat}(t) = E_{bat}(t-1)(t-\sigma) + (\frac{E_{bat}(t)}{\eta_{inv}} - E_s(t)) \quad \text{(III.11)}$$

III.7. Sizing of the conversion system (converter)

III.7.1. Functional analysis of the bidirectional converter

The bidirectional converter connects the DC and AC buses, providing conversion in both directions. It functions as an inverter (DC → AC) and a rectifier (AC → DC), improving the reliability and energy efficiency of the system (figure.III.6).

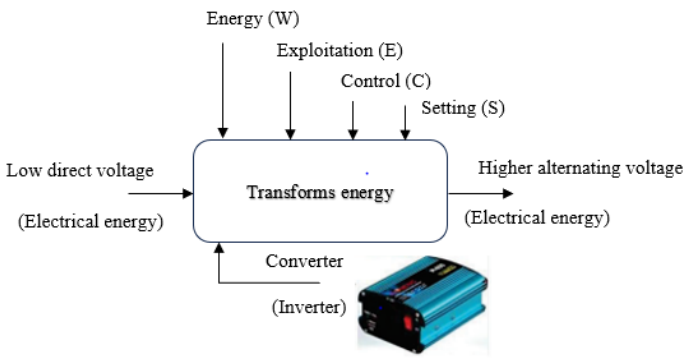

Figure III.6. Functional analysis of a converter.

The inverter yield (η_{inv}) depends on the load, specifically the AC output power ($P_{0,inv}$), forming what is known as the inverter load curve. For analysis, the yield must be expressed based on the DC input power. Electrical losses can be approximated by a constant component, p_0, independent of the load. It is necessary to express the yield as a function of the input power.

Reduced electrical losses P_{losses}, can be expressed their expression is presented as follows:

$$P_{losses} = \frac{P_{losses}}{P_{inv}} = P_o + k.P^2 \quad \text{(III.12)}$$

P_{losses} = Electrical losses [%];

P_{inv} = Nominal power of the inverter [%];

P_o and k = Coefficients calculated from the data provided by the manufacturer, by equations III.13 and III.14:

$$P_o = \frac{1}{99}\left(\frac{10}{\eta_{10}} - \frac{1}{\eta_{100}} - 9\right) \quad \text{(III.13)}$$

$$k = \left(\frac{1}{\eta_{100}}\right) - P_o - 1 \quad \text{(III.14)}$$

Or:

η_{10} and η_{100} are the yields at 10% and 100 % load, respectively, relative to the nominal power given by the manufacturer.

The reduced power p_{red}, also called load factor τ_{inv}, is expressed as:

$$\tau = P_{red} = \frac{P_{O,inv}}{P_{inv}} \quad \text{(III.15)}$$

Or:

$P_{O,inv}$ = Inverter output power [kW].

Electrical losses are the difference between the input DC power $P_{E,\,inv}$ et the output power:

$$P_{losses} = P_{I,inv} - P_{O,inv} \quad \text{(III.16)}$$

Thus, by combining equations III.12 and III.16, we obtain:

$$(P_o + k.P^2).P_{inv} = P_{I,inv} - P_{O,inv} \quad \text{(III.17)}$$

On the other hand, input power can be expressed from output power and efficiency:

$$P_{I,inv} = \frac{P_{O,inv}}{\eta_{inv}} \quad \text{(III.18)}$$

Thus, after substituting III.18 into III.17 and using III.16, we obtain the equation:

$$P_o + k.P^2 = \frac{P}{\eta_{inv}} - P \quad \text{(III.19)}$$

Hence the inverter's yield:

$$\eta_{inv} = \frac{P}{P+P_0+k.P^2} \quad \text{(III.20)}$$

Today, the best inverters reach peak efficiencies of 98% and the average is 95.2% [29].

III.8. Sizing of the MPPT converter

III.8.1. MPPT converter

By continuously tracking and operating at the maximum power point, the MPPT is an essential component of increasing a photovoltaic system's power output. Under different temperature and irradiance conditions, it improves system efficiency (figure III.7).

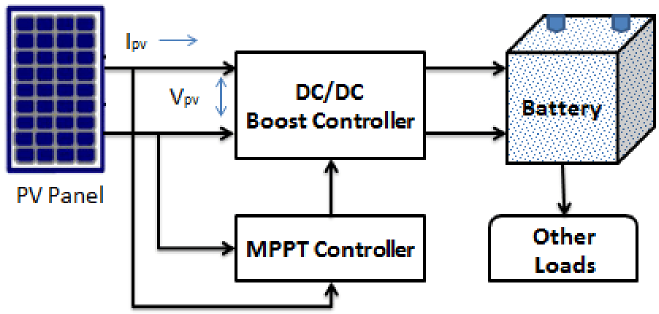

Figure III.7. Block diagram of MPPT controller [30].

Maximum power admissible by the MPPT [31]:

$$P_{MPPT} \geq P_{PV,max} = N.P_m \quad \text{(III.21)}$$

Or:

P_{MPPT}= Nominal power of the MPPT converter;

N= Total number of PV modules;

P_m= Peak power of a module (W).

Maximum input voltage (in cold conditions) [32, 33]:

$$U_{PV,max} \geq N_S.U_{oc,m,max} \quad \text{(III.22)}$$

Or:

N_S= Number of modules in series;

$U_{oc,m,max}$= The maximum open-circuit voltage of the module (minimum temperature).

Maximum input current [32, 34]:

$$I_{PV,max} = N_P . I_{sc,module} \tag{III.23}$$

Or:

N_p= The number of branches in parallel;

$I_{sc,module}$= The short-circuit current of the module.

III.9. Conclusion

This chapter displays the dimensions of the components used in the hybrid PV/DG system. The functional analysis, technique method allows you to conceal a viable and adaptable system, in view of its global performances.

Chapter IV

Results and analysis

IV.1. Introduction

Using HOMER Pro, this study evaluates hybrid PV/DG with battery storage systems for El Hadjadj. Technical and economic performance is used to compare different configurations, including grid extension. The purpose is choosing the most economical and effective way to ensure a steady supply of energy.

IV.2. HES modeling and optimization flowchart

The approach used to identify the optimal HES for the study area is illustrated in the flowchart shown in figure IV.1.

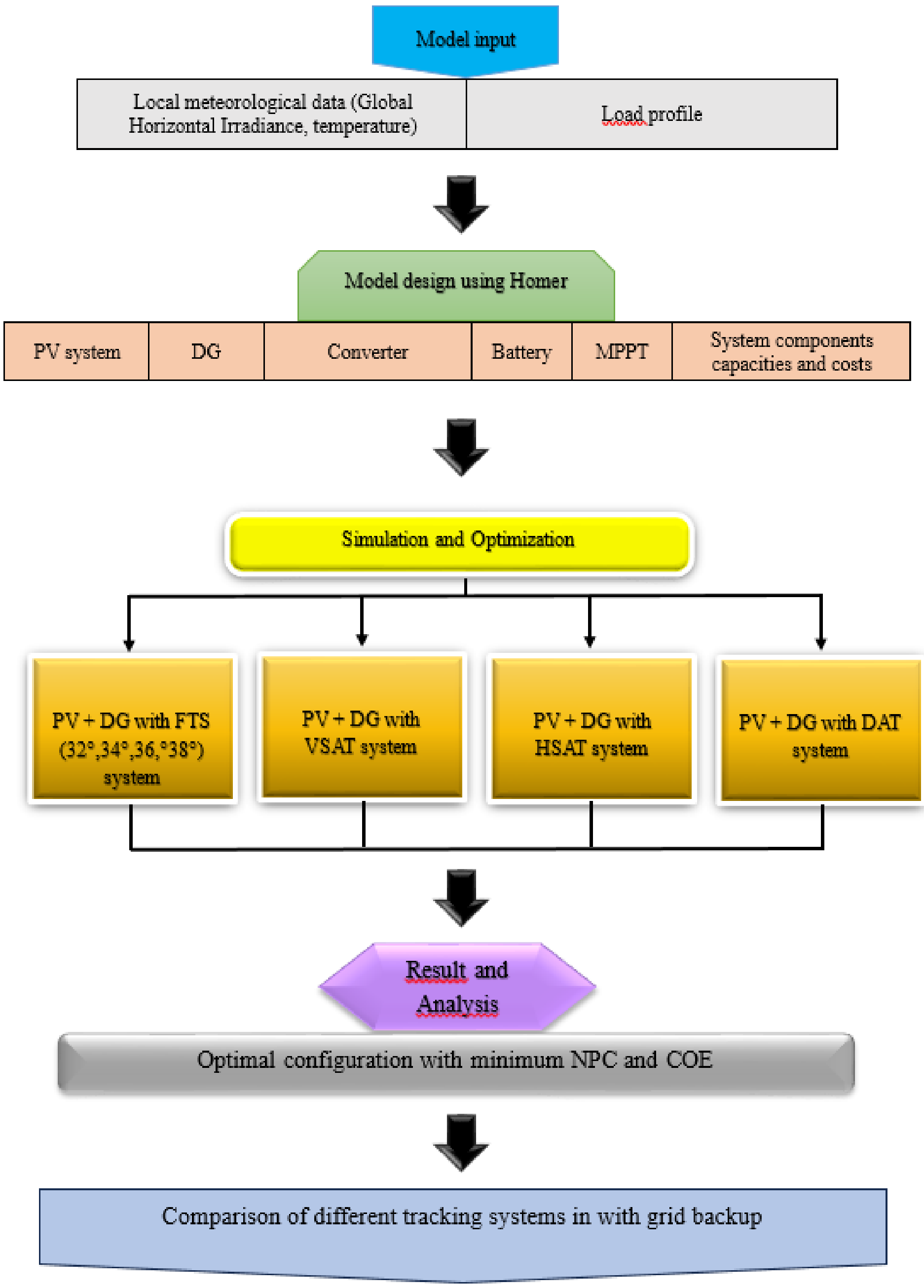

Figure IV.1. Flowchart describing the optimization and modeling stages for the design of the HES.

IV.3. Presentation of the HOMER pro software

HOMER software enables the design and analysis of HES. It combines renewable or conventional sources, storage and load management, with or without a grid connection. HOMER takes into account technical and economic aspects to determine the optimal solution. It performs simulation, optimization and sensitivity analysis throughout the project's lifetime.

IV.4. Dimensioning by HOMER pro software

IV.4.1. Geographical location

The rural commune of El Hadjadj, located 210 km southwest of Algiers in Chlef, benefits from strong solar potential due to high annual sunshine. Isolated from the electricity grid (figure IV.2).

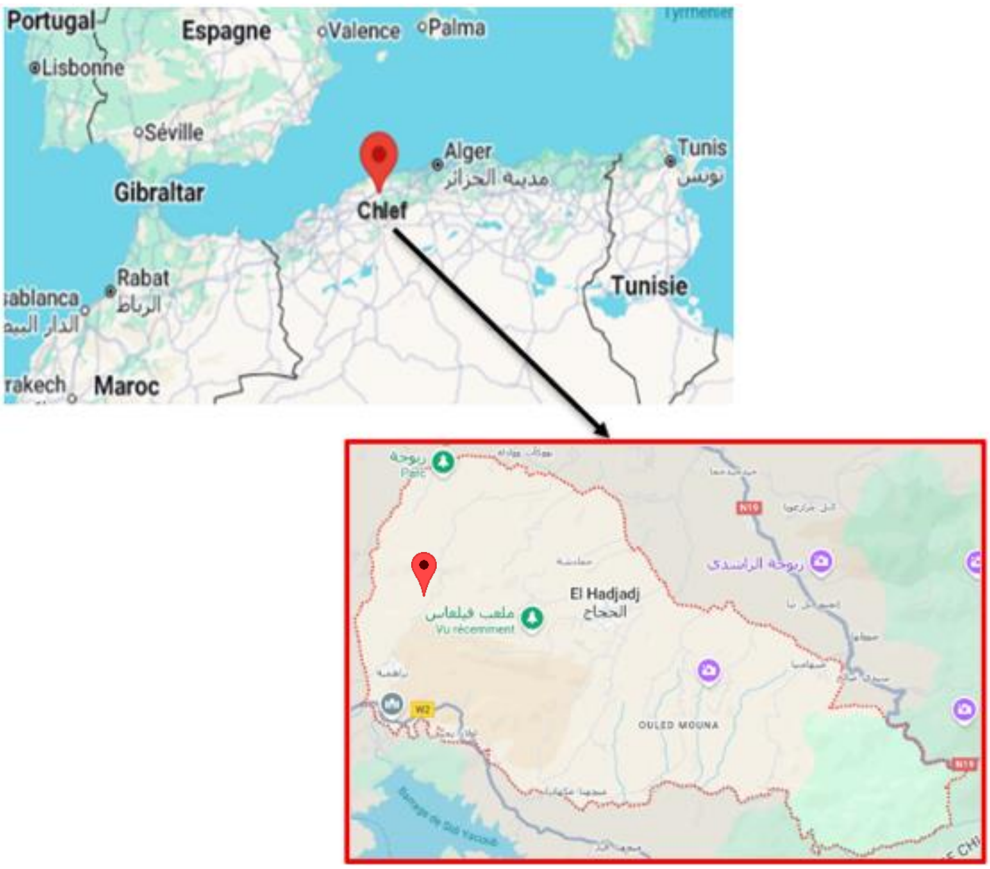

Figure IV.2. Geographical location of the study the house (El Hadjadj, Chlef).

IV.4.2. Climate data

El Hadjadj has a semi-arid Mediterranean climate, the monthly temperature profile in figure IV.3 shows mild winters and hot summers, with temperatures around 10.37°C in January and 11.59°C in December. Summer temperatures peak at 27.57°C in August, with an annual average of 18.18°C.

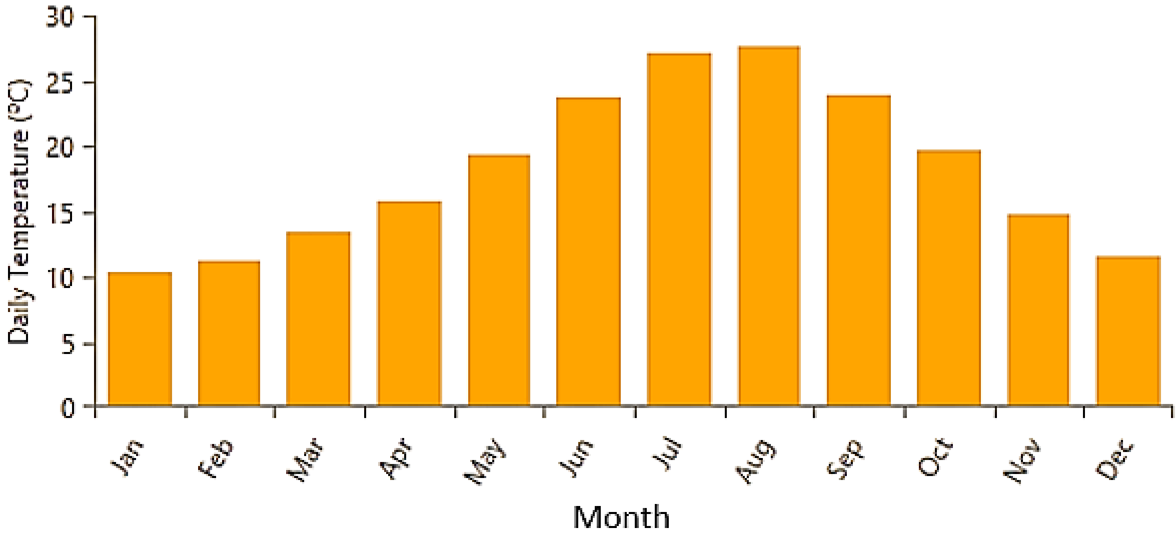

Figure IV.3. Represents the monthly temperature of the site.

This climate is favoring strong solar energy potential that is well suited for efficient year-round PV performance especially during the hot sunny months.

IV.4.3. Irradiance of the study site

With a clearness index of 0.525 to 2.36 kWh/m²/day in December, the site has low solar radiation during the winter months. June sees the highest solar potential, with a clearness index of 0.648 to 7.49 kWh/m²/day (figure IV.4).

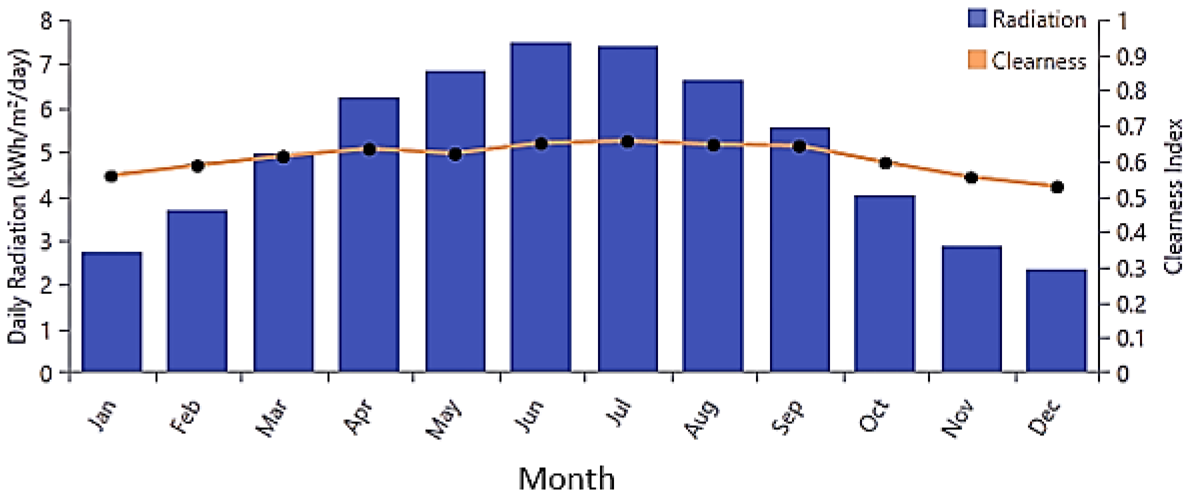

Figure IV.4. The variation of average solar irradiation.

The numbers show that the spring through summer months are ideal for PV generation.

IV.4.4. Load Profile

The figure IV.5 reveals stable electricity demand throughout the year, with occasional increases in summer and winter of around 3.2 kW. These seasonal fluctuations reflect increased thermal needs. They guide the efficient sizing of the hybrid system.

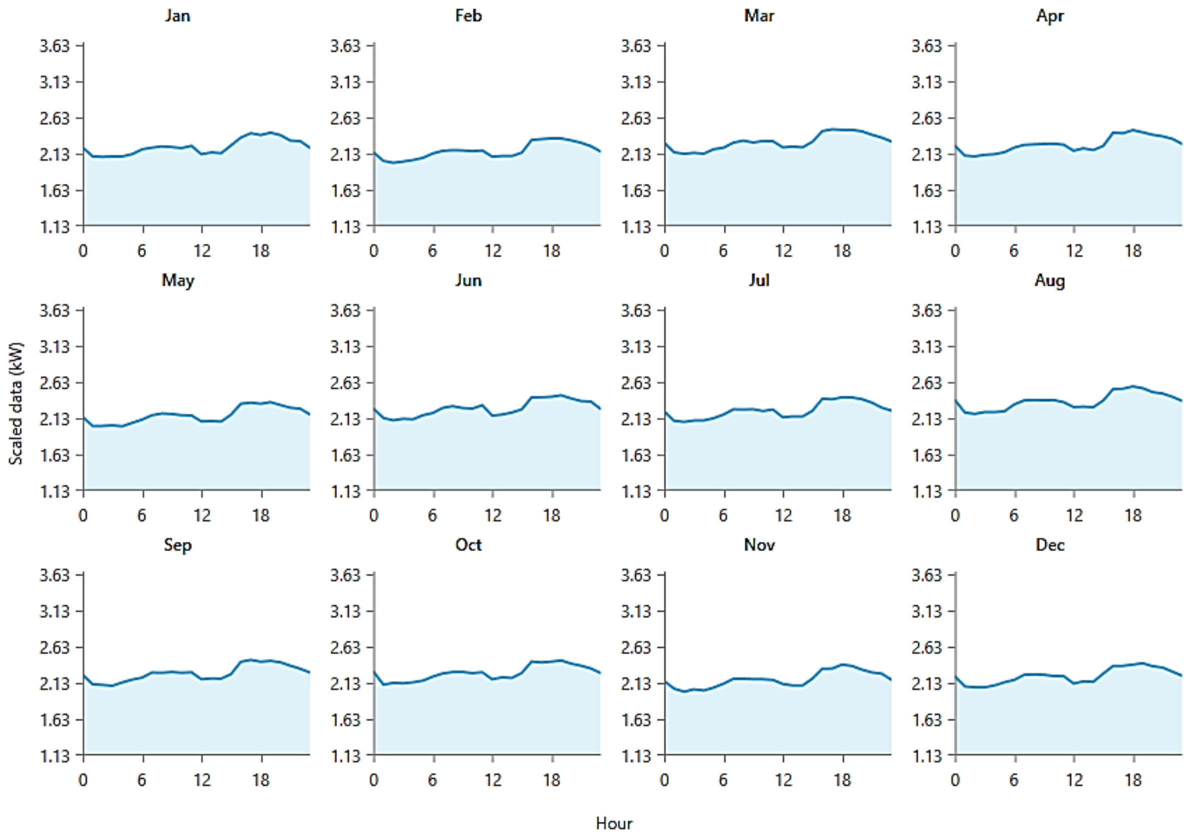

Figure IV.5. Electrical load.

IV.5. Technical - economical parameter of components for our study

The key component costs and specifications of (PV, DG, converter, battery and MPPT) are detailed in Tables IV 1 to five. These data support a 25-year simulation using Homer software.

Table IV 1: PV parameters [35,36].

PV	
Model name	CEM100M-36
Capacity (kW)	1
Capital cost (US$)	796
Replacement cost (US$)	796
Operation & maintenance cost (US$/y)	0
Operating temperature (°C)	25
αp (%/◦C)	-0.41
Efficiency (%)	13
Life time (y)	25

Table IV 2: DG parameters [37].

DG	
Model name	1 kW GMI
Capacity (kW)	1
Min. load ratio (%)	30
Life time (h)	3650
Fuel	Diesel
Capital cost (US$)	342
Replacement cost (US$)	342
Operation & Maintenance cost (US$/y)	0.05
Fuel price (US$/L)	0.7 [38]

Table IV 3: Converter parameter [39].

Converter	
Capacity (kW)	1.6
Capital cost (US$)	546
Replacement cost (US$)	546
Operation & maintenance cost (US$/y)	7
Efficiency (%)	82
Life time (y)	25

Table IV 4: Battery parameters [39].

Battery	
Model name	Hoppecke 16 OPzS 2000
Nominal Capacity (kWh)	4.76
Roundtrip efficiency (%)	86
Min. state of charge (%)	30
Capital cost (US$)	276
Replacement cost (US$)	276
Operation & Maintenance cost (US$/y)	20
Throughput (kWh)	6737.40
Life time (y)	20

Table IV 5 : MPPT parameter.

MPPT	
Capacity (kW)	6
Capital cost (US$)	900
Replacement cost (US$)	720
Operation & maintenance cost (US$/y)	10
Efficiency (%)	98
Life time (y)	20

Solar panels are typically installed at a fixed tilt, but tracking systems can improve energy capture by following the sun's path. This study examines four such tracking systems, shown in figure IV.6.

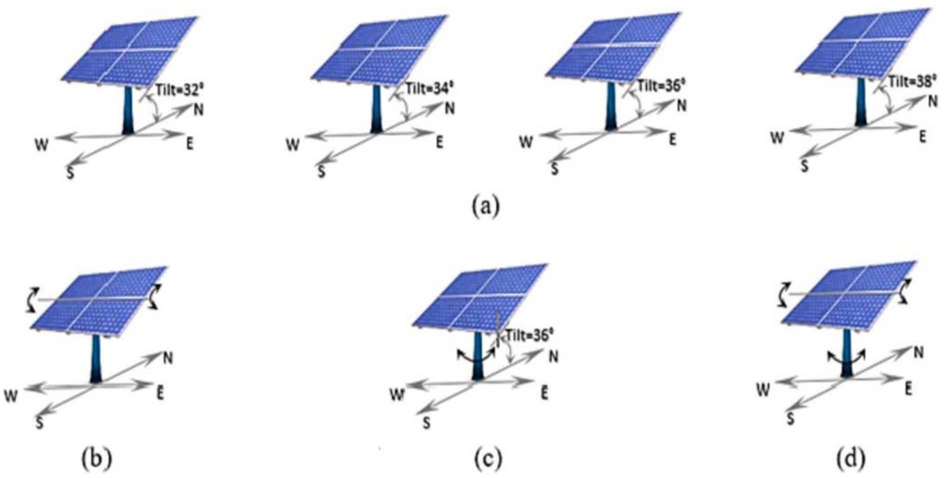

Figure IV.6. PV tracking systems (a) Fixed-facing at four different tilt angles (b) Horizontal single-axis solar tracker (c) Vertical single-axis solar tracker (d) Dual axis tracker [40].

1. Fixed-tilt solar panel (FTS) as shown in figure. IV.7 (a);
2. Horizontal single-axis tracking (HSAT) as shown in figure IV.7 (b);
3. VSAT or vertical single axis tacking as shown in figure IV.7 (c);
4. DAT or Dual Axis Tracker as shown in figure IV.7 (d).

Different tracking systems costs are given in Table IV 6.

Table IV 6: Tracking systems cost [41].

Tracking system	Capital cost ($/kW)
FTS	0
HSAT	870
VSAT	255
DAT	1000

IV.6. Results and discussion

IV.6.1. Technical comparison between different tracking systems

IV.6.1.1. Energy production and excess

This study compared several photovoltaic systems, including FTS, HSAT, VSAT, and DAT systems. The DAT system produced the most energy (37788 kWh/year) and had the greatest surplus (12167 kWh/year). Advanced monitoring systems showed a clear superiority in terms of energy efficiency (figure IV.7).

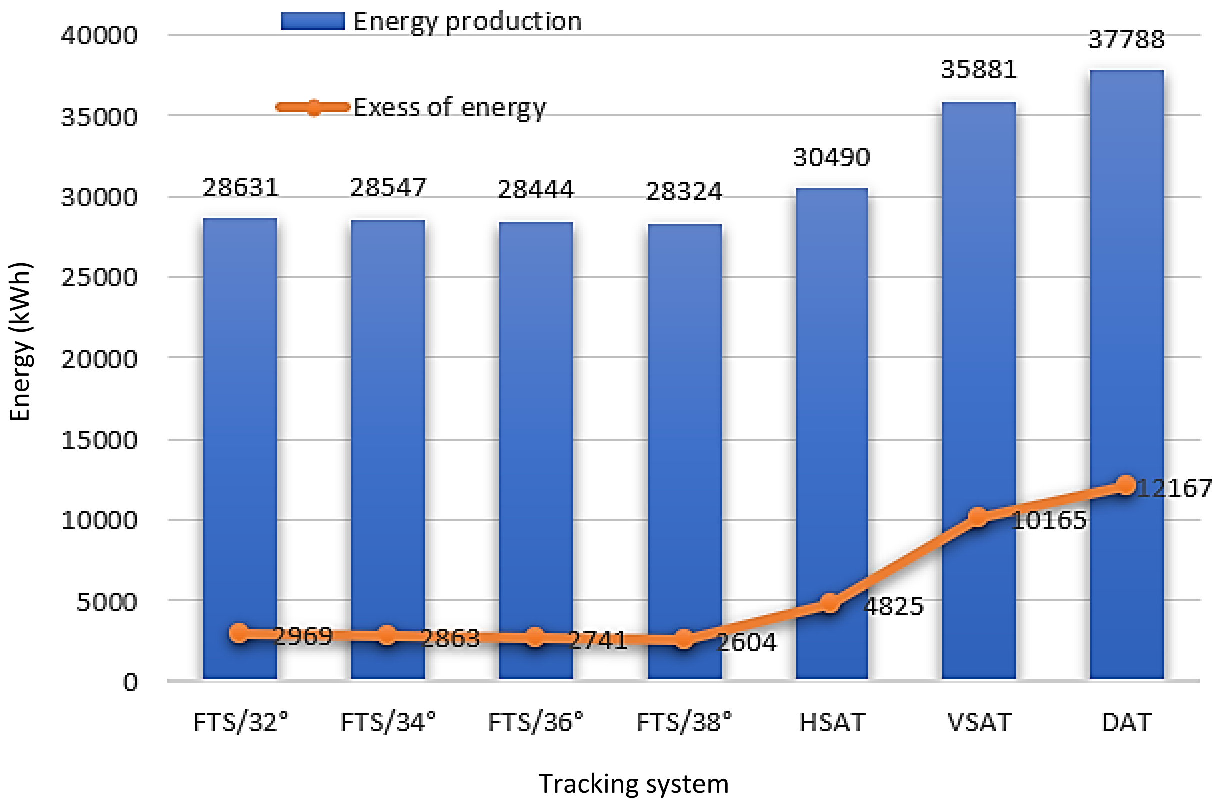

Figure IV.7. Energy production and excess of one year for different PV tracking techniques.

IV.6.1.2. PV penetration

The photovoltaic systems increase the energy consumption of the complex. The DAT comes with a penetration of 192%, compared 141% to 153% for other configurations. These systems are automated and compatible with diesel generators (figure IV.8).

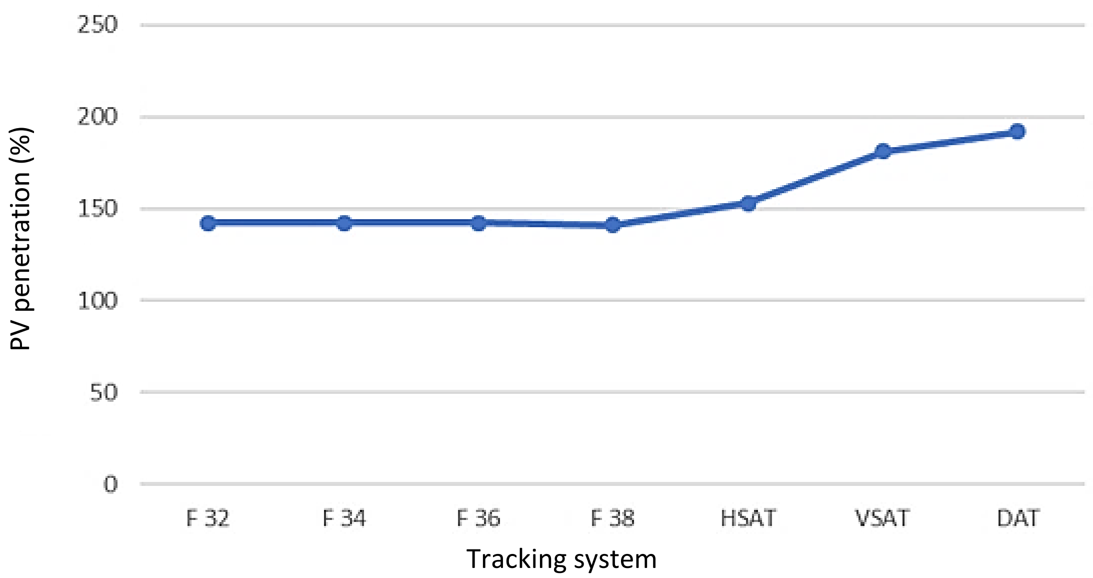

Figure IV.8. PV penetration of one year for different PV tracking techniques.

IV.6.1.3. Capacity factor

DAT has the highest capacity factor (28.7%), followed by VSAT (27.1%), while all FTS systems have the lowest (21.2% to 21.3%) as shawn in figure IV.9.

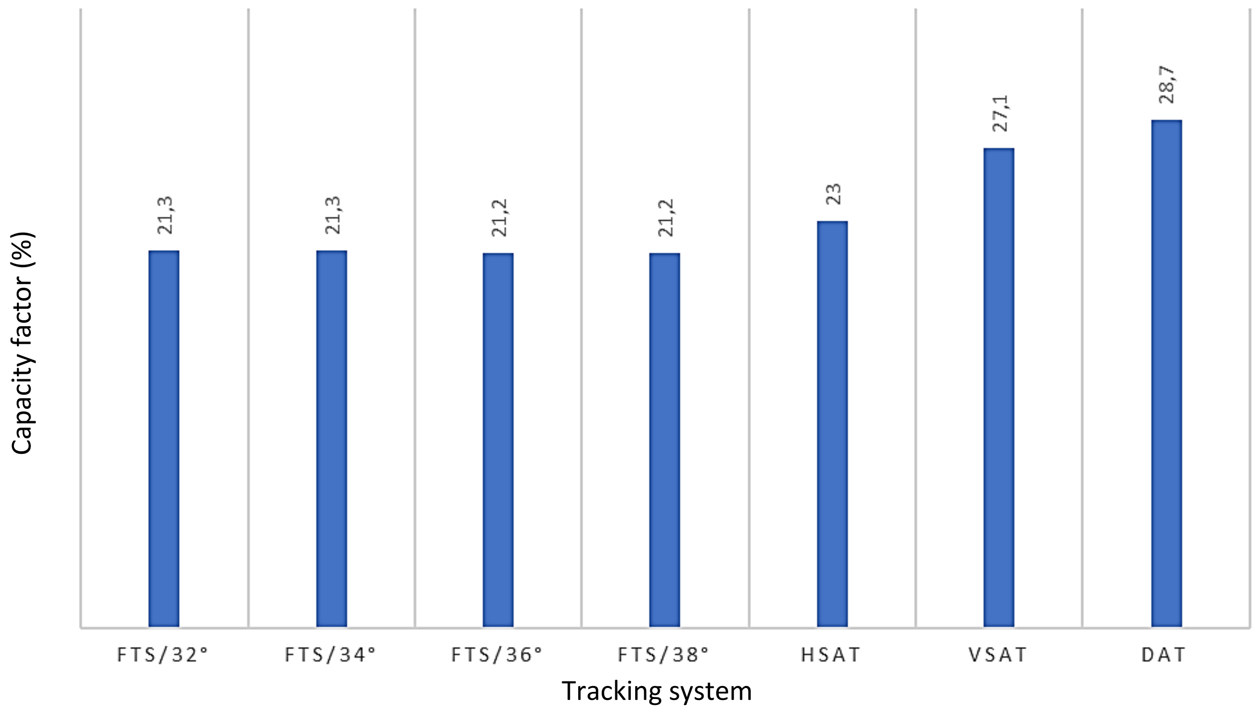

Figure IV.9. Capacity factor for different PV tracking techniques.

The capacity factor in tracking systems is known as the ratio of actual energy production to the maximum achievable.

IV.6.1.4. Impact of MPPT on performance

By getting in more power, MPPT increases PV output, as indicated by the blue curve above the yellow curve figure IV.10. It adjusts to changes in temperature and irradiance to maintain maximum efficiency. On days with changing weather, this effect is most evident.

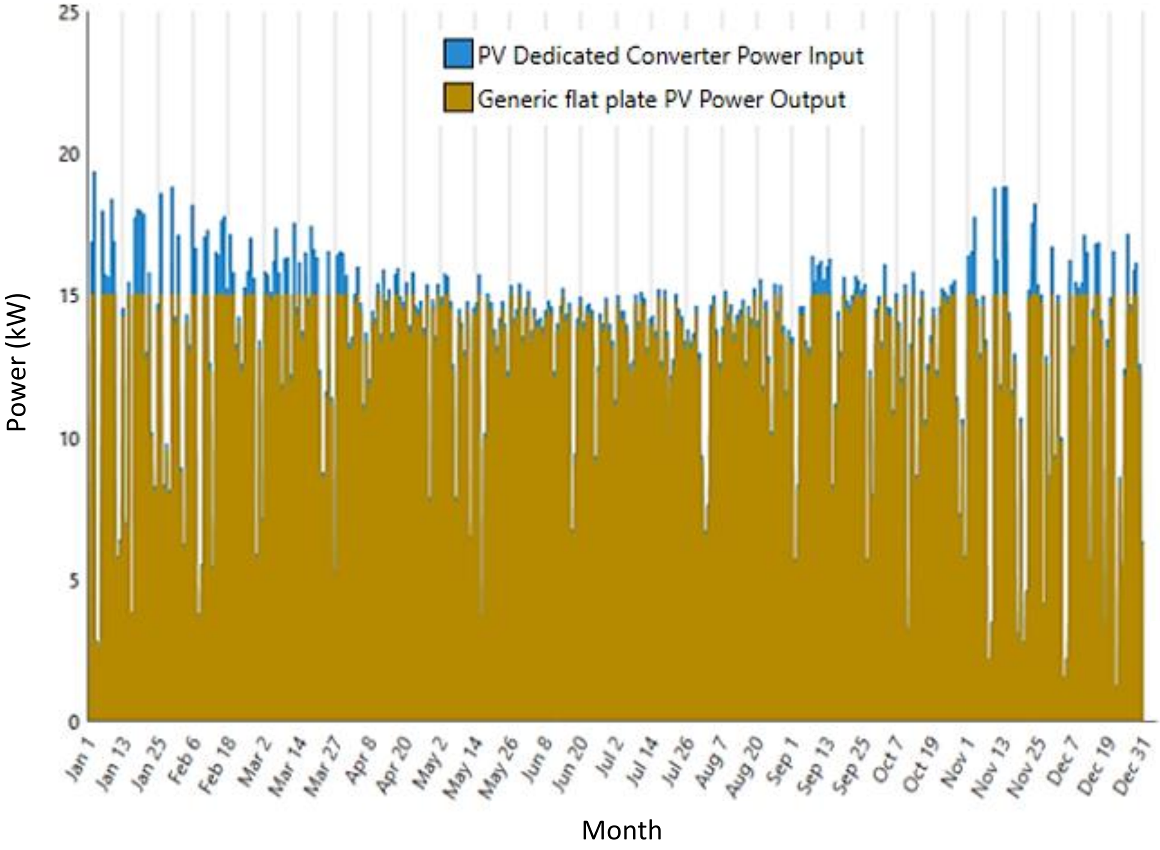

Figure IV.10. Daily power comparison between PV and MPPT converter.

IV.6.1.5. Monthly generation

Based on technical analysis, the DAT system was found to be the most efficient and productive of the four PV tracking options at the studied site. With a capacity of 37788 kW of PV and 32.5 kW of DG power, the system generates 99.9% of its annual electricity from PV and 0.0860% from DG. Figure IV.11 shows the monthly energy contribution of each system component.

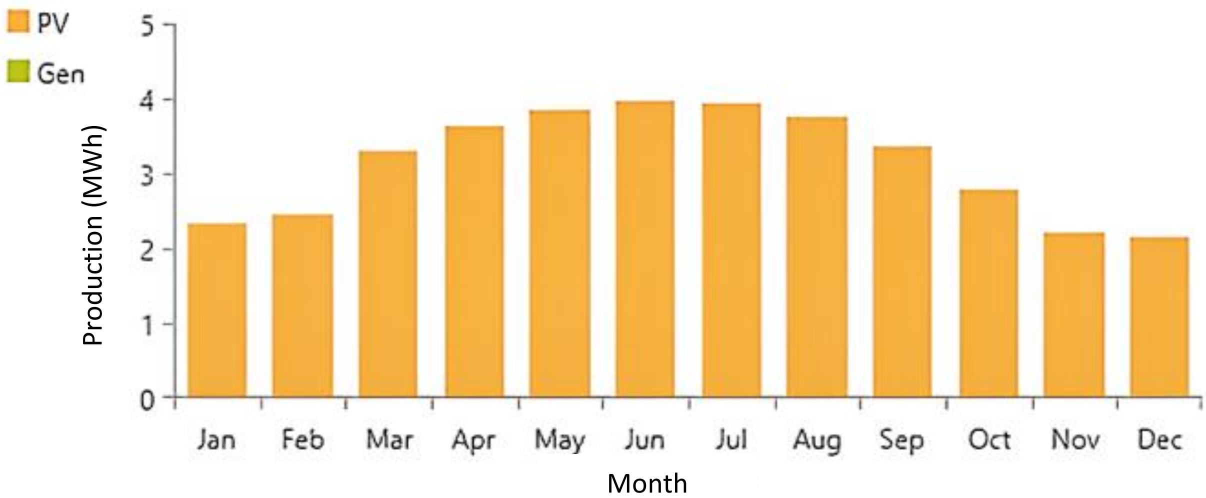

Figure IV.11. Monthly generation of the PV/DG system.

IV.6.2. Economic analysis

The results of the economic analysis, including the net present value NPC and COE for each configuration are presented in Table IV 7.

Table IV 7: Results for HES.

Scenario \ Parameter	PV [kW]	DG [kW]	Battery [hr]	Converter [kW]	NPC [$]	COE [$/kWh]
FTS/38°	15	485	133	3.88	21985	0.0863
FTS/36°	15	538	133	3.88	22364	0.0878
FTS/34°	15	600	133	3.88	22872	0.0898
FTS/32°	15	670	133	3.91	23396	0.0918
VSAT	15	242	105	3.88	23791	0.0934
HSAT	15	261	132	3.88	33441	0.131
DAT	15	32.5	133	4.00	34049	0.134

DAT has the highest NPC and COE due to the high cost of the tracking system (1000 $/kW). By reducing it we obtain the lowest cost configuration, wich is FTS/38° hybrid system with an NPC of 21985$ and a COE of 0.0863$/kWh. Figure IV. 12 shows the cost of each component of this system.

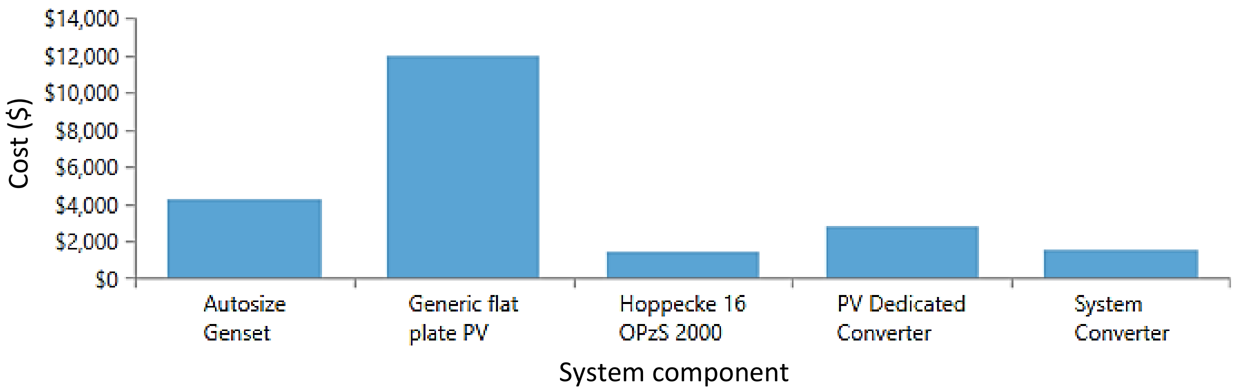

Figure IV.12. Cost breakdown of various components of FTS/38° hybrid system.

In order to rank different energy system configurations, Homer computes the NPC and COE primary economic metrics. The NPC subtracts the current revenues from the present cost of installing and maintaining the system over the course of the project, and the result is provided by:

$$NPC = \frac{C_{ann,tot}}{CRF(i,N)} \quad \text{IV.1}$$

Or :

- $C_{ann,\,tot}$ = total annualized cost [$/y];
- N = projet life time [y];
- i = annual interest rate [%].
- CRF = capital recovery factor and it is calculated by the following equation:

$$CRF(i, N) = \frac{i(1+i)^N}{(1+i)^N - 1} \quad \text{IV.2}$$

The COE is known as the average price per unit of energy (kWh). To determine it HOMER uses the following equation:

$$COE = \frac{C_{ann,tot}}{E_{tot}} \quad \text{IV.3}$$

Where:

- E_{tot} = total electricity served to the load annually (kWh/y).

IV.6.2.1. Cash flow by component and cost type

The cash flows of the optimal hybrid system detailed by component and cost type. Figures IV.13 (a) represents the initial cost of total investment at installation, including PV generators, the solar tracker, Hoppecke batteries, flat PV modules, the generator set, hydrogen storage and converters. Figure IV.13 (b) shows the evolution of the flow over 25 years, highlighting a significant initial investment, followed by operating costs and a recoverable residual value at the end of the system's life.

(a)

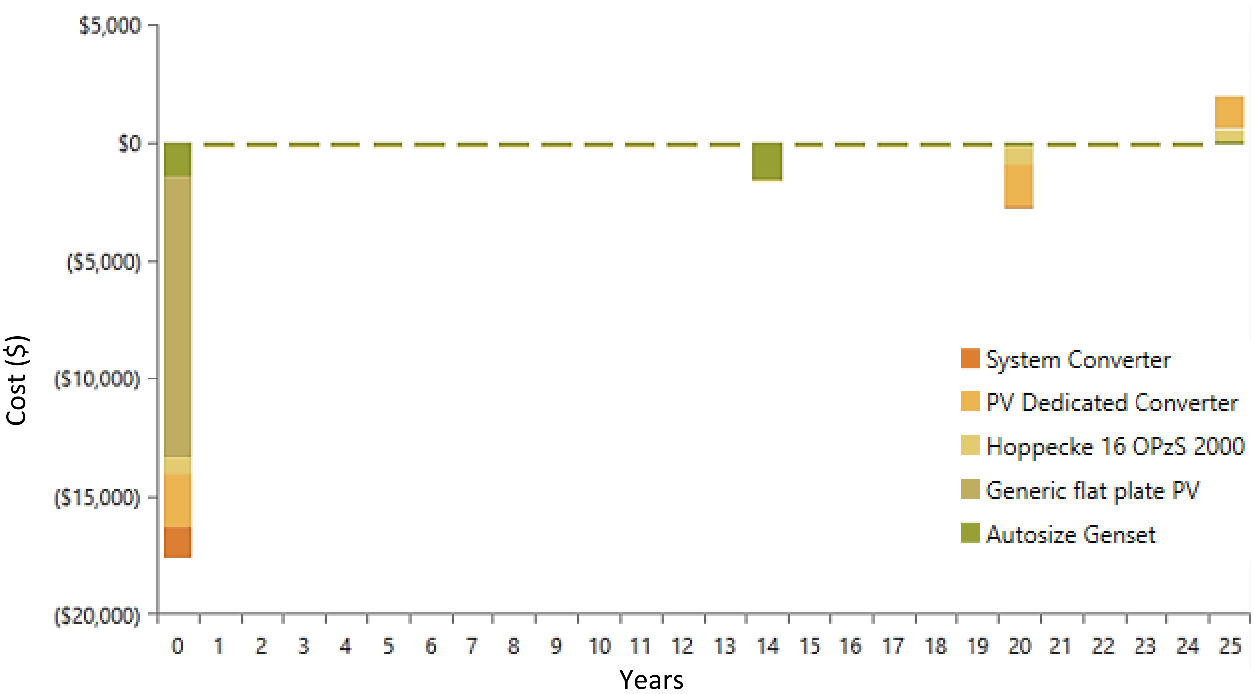

(b)

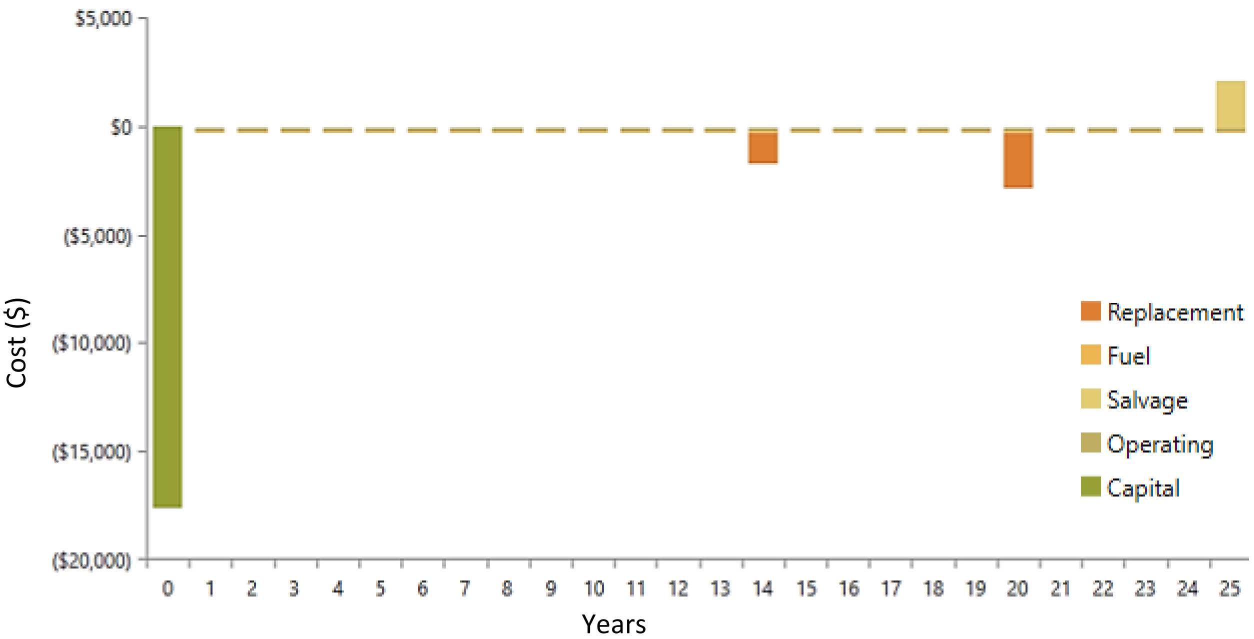

Figure IV.13. Cash flow of the optimum system listed by (a) component, (b) cost type.

IV.7. Operation status of the optimal PV tracking technique (FTS/38°)

IV.7.1. PV electrical summary

The hourly power output over a year is depicted in figure IV.14, with peak production occurring between 9:00 and 18:00 and reaching up to 15 kW during sunny periods. The FTS/38° system continues to function steadily in spite of daily and seasonal variations. With an average output of 3.18 kW, 76.3 kWh of energy are produced daily.

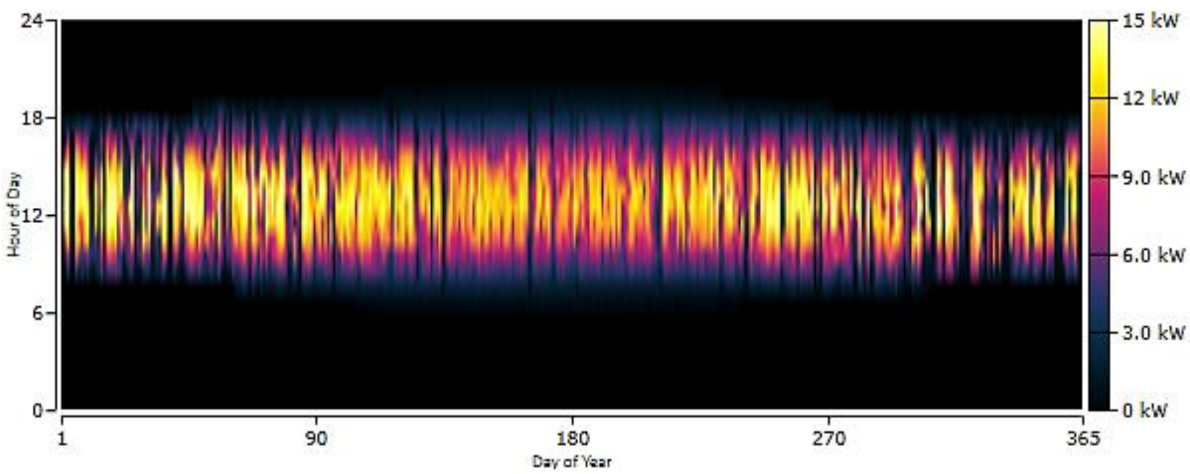

Figure IV.14. PV power output throughout the year for the FTS/38° system.

IV.7.2. DG electrical summary

Is used in a very limited way, which reflects the relevance of the overall sizing of the system. It only intervenes in case of emergency, with only 263 h of operation per year. Its contribution to electricity production is low (485 kWh/y), as is its fuel consumption (175 L/y). (Figure IV.15).

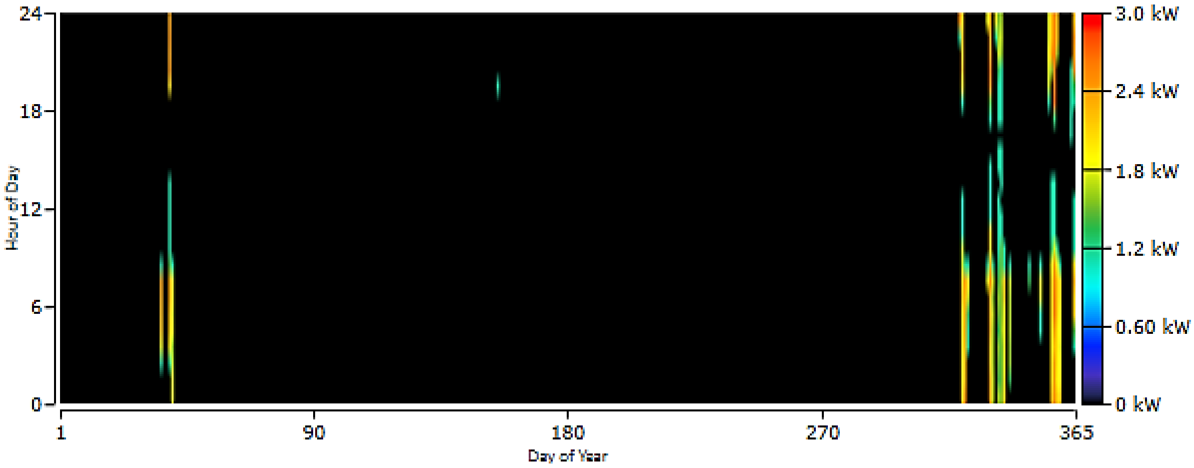

Figure IV.15. DG power output throughout the year for the FTS/38° system.

Chart figure highlights the low demand on the generator, mainly observed at the end of the year, when photovoltaic production and battery storage are no longer sufficient to meet demand. This trend underlines a minimal dependence on diesel.

IV.7.3. Battery storage

Throughout the year, the battery stored the electrical energy produced to ensure the continuity of the system and the supply of the necessary energy to the house (figure IV.16).

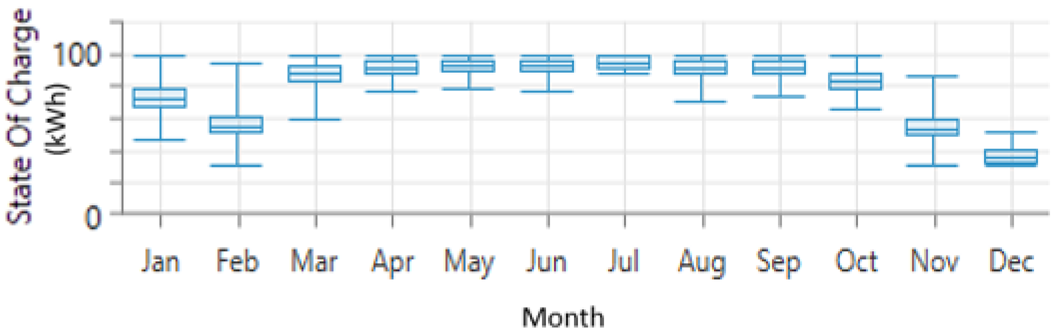

Figure IV.16. State of charge over one year.

The batteries have a capacity of 428 kWh, its input energy is 15172 kWh/y, its output energy is 13326 kWh/y and its losses are 2146 kWh/y. A lifetime flow rate 287394 kWh.

IV.7.4. Converter electrical summary

The optimal converter power was estimated at 3.88 kW. Figure IV.17 illustrate the annual utilization of the converter, highlighting its role in the overall operation of the system.

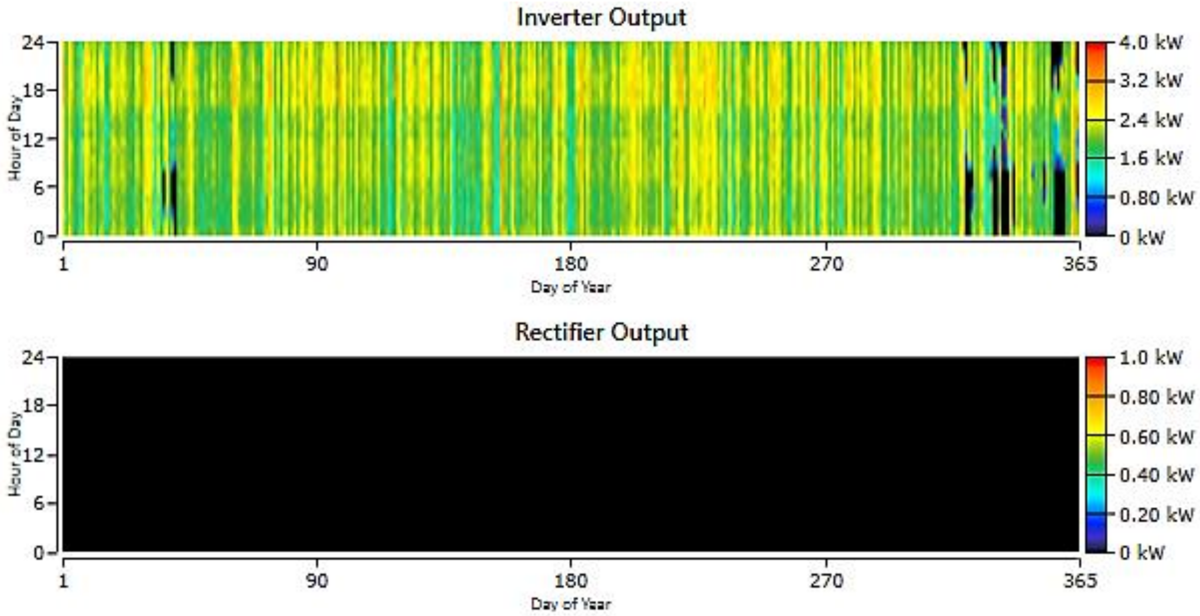

Figure IV.17. FTS/38° system converter.

The inverter generates a steady output of 2.19 kW (56.6% of its 3.88 kW capacity), while operating almost (8607 hours per year). It converts 23446 kWh/y of input energy into 19225 kWh/y of useful output. Its efficiency in preserving system performance is demonstrated by the total conversion losses, which come to 4220 kWh/y annually.

The rectifier output is blank, indicating that the rectifier was not used. Energy therefore flows only from DC to AC.

IV.7.5. Renewable penetration

This graph (figure IV.18) shows the real-time share of energy demand met by renewable sources. It provides a scalable, hourly indicator to assess how effectively renewables meet the system load throughout the year.

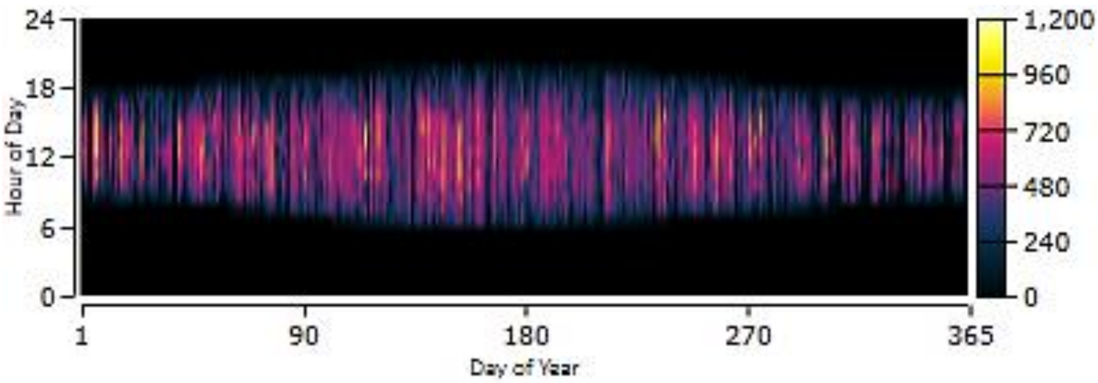

Figure IV.18. Instantaneous renewable output divided throughout the year for the FTS/38° by load.

The colors show the ratio between renewable production and consumption. Light areas indicate excess energy that can be stored or lost, while dark areas show a deficit of production compared to demand.

IV.8. Grid extension electrification cost

Figure IV.19 illustrates that when the distance crosses approximately 0.26 km, FTS/38° becomes more economical than grid extension. The standalone system is a better investment because its cost remains constant however, grid extension costs rise linearly with distance.

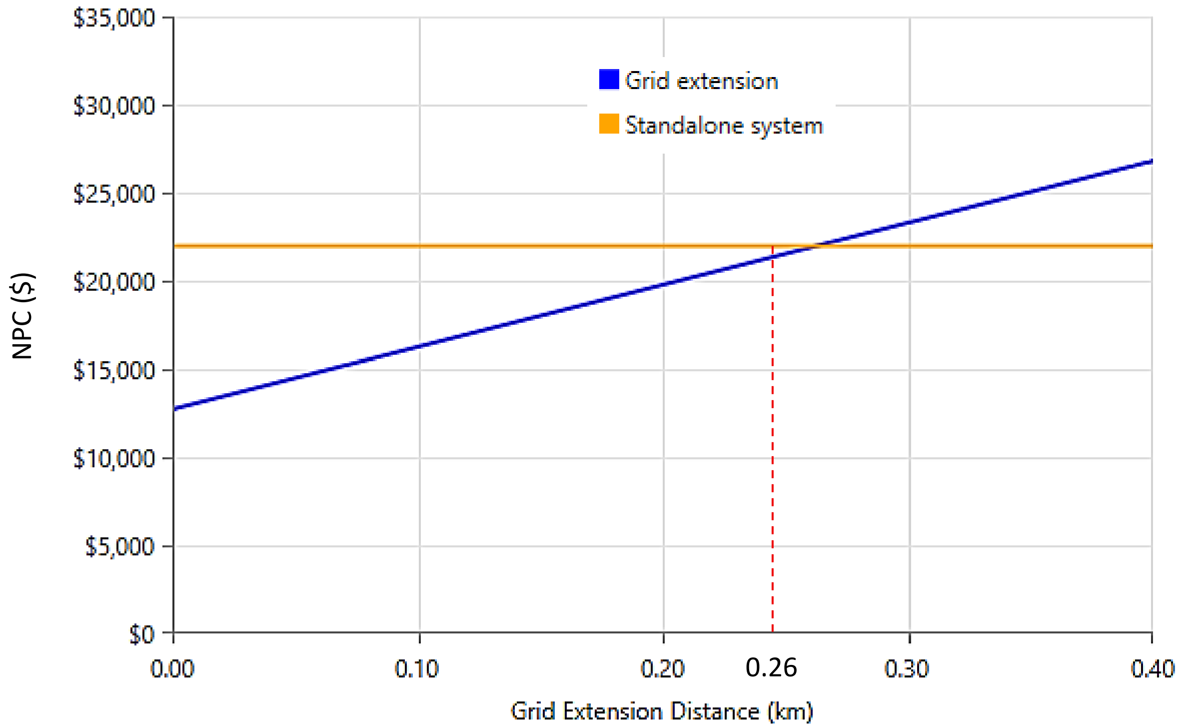

Figure IV.19. NPC for FTS/38° and grid extension as function of distance.

This makes investment beyond short distances better and highlights the economic advantage of autonomous systems in rural areas.

IV.9. Conclusion

This chapter analyzed hybrid PV/DG with battery storage systems for El Hadjadj using Homer Pro, underline the impact of configuration choices on performance. With the lowest NPC, the analysis finds that economically the FTS/38° is the most practical choice even when compare it to grid extension, and technically DAT is better.

General conclusion

General conclusion

In order to deal with the energy requirements of isolated regions, a standalone HES that combines PV, DG, and a battery storage system has been successfully researched, sized, and simulated in this work.

Chapter 1 proved that the transition to renewable energy sources is crucial due to the limited availability of fossil fuels and their increasing consumption resulting from the growing global demand for energy.

Chapter II verified that photovoltaic technology is a practical and promising solution due to Algeria's large solar energy potential. The potential for increasing energy capture and system efficiency was brought to light by the study of PV technologies.

Chapter III provided a detailed technical sizing of the HES, demonstrating how a properly sized set of PV panels, DG, batteries, and an MPPT which is essential to ensure the efficiency and profitability of a photovoltaic installation, especially in variable environments.

Chapter IV shown the HOMER Pro software simulation results, which demonstrated that the suggested HES could keep steady energy delivery while greatly reducing fuel consumption and operating expenses.

Chapter IV presents the HOMER Pro software simulation results, which demonstrated that the DAT system achieved the highest energy production, while the FTS/38° system offered the best economic performance.

The results of this study demonstrate the foundation for future developments and practical applications in Algeria and similar contexts, and they illustrate that hybrid systems are both financially and technically possible as a sustainable energy source for remote regions.

References

[1] Priyam Study Centre. *"Non-renewable energy resources: crude oil, coal, natural gas, and nuclear fuel"*.https://www.priyamstudycentre.com/wp-content/uploads/2022/12/Non-renewable-energy-resources-crude-oil-coal-natural-gas-and-nuclear-fuel-300x240.png

[2] Clean Energy Group. *"Fossil fuels and their impact"* https://www.econnectenergy.com/articles/the-benefits-of-gas-to-power

[3] DTE Energy. *"Coal-fired power plant image"*.https://s7d1.scene7.com/is/image/dteenergy/Coal_800x300

[4] ETPA. *"Combustion turbine diagram"*. https://www.etpa.nl/knowledge-base/technology/oil-fired-energy-generation

[5] Nuclear Power. *"Nuclear power plant process (GIF)"*. https://nuclear-power.com/wp-content/uploads/2014/10/Nuclear_Plant.gif

[6] M.N.Mchalikh et CH.Hmada''Modélisation et simulation d'un système photovoltaïque en fonctionnement autonome et connecté au réseau '' Mémoire de Master Université Kasdi Merbah–Ouargla 2013.

[7] انرژی گرمایی (énergie thermique). https://www.jahaneshimi.com/10435/انرژی-گرمایی/

[8] Quizlet. *"Types of renewable energy - diagram"*. https://o.quizlet.com/qAr6kTY19KiUEHKjRpypaA.jpg

[9] Greenesa. *"Detailed geothermal energy system"*. https://greenesa.com/uploads/news/1631205661Geothermalenergydetailgreenesa.png

[10] Energy Education. *"Dam parts - hydropower structure"*. https://energyeducation.ca/wiki/images/thumb/8/8e/Damparts.png/780px-Damparts.png

[11] Image générique sur les barrages. https://encryptedtbn0.gstatic.com/images?q=tbn:ANd9GcTk50qgFzl2I_FCCO20QfX0uxyDFZ5NjlLd1Q&s

[12] Énergie solaire vs énergies fossiles : le duel écoresponsable https://www.sadel-photovoltaique.com/wp-content/uploads/2025/03/energie-solaire-vs-fossiles-1024x512.png

[13] Unex. *"Global energy distribution map"*. https://solutions.unex.net/wp-content/uploads/2023/06/mapa-unex-scaled.jpeg

[14] BOUZERIA HAMZA , ZOUITEN ISSAM "ètude des hacheurs et leurs applications dans l'optimisation des generateurs photovoltaique" Mémoire de mastre d'electrotechnique, Universitè badji mokhtare annaba,2011.

[15] ResearchGate. *"Principe de fonctionnement d'une cellule photovoltaïque"*. https://www.google.com/url?sa=i&url=https%3A%2F%2Fwww.researchgate.net%2Ffigure%2FPresentation-schematique-dune-cellule-solaire-

5_fig2_329980090&psig=AOvVaw02UJcebxPuc_8Bd5T2_Hns&ust=1751130264702000&source=images&cd=vfe&opi=89978449&ved=0CBAQjRxqFwoTCMir4NyKko4DFQAAAAAdAAAAABAE

[16] TPE - Panneaux Photovoltaïques. *"Fonctionnement et types de panneaux photovoltaïques"*. http://tpe-panneauxphotovoltaiques.e-monsite.com

[17] Wikiwater. *"Schéma explicatif de panneau solaire thermique ou photovoltaïque"*. https://wikiwater.fr

[18] ResearchGate – Abdelkader Mahmoudi. *"Caractéristique résultante d'un groupement de n-p cellules en parallèle"*.https://www.researchgate.net/publication/327839184

[19] Sadel Photovoltaïque. (s.d.). *Comparaison entre l'énergie solaire et les énergies fossiles*. Consulté le 30 juin 2025, sur https://www.sadel-photovoltaique.com/energie-solaire/comparaison-entre-lenergie-solaire-et-les-energies-fossiles

[20] B. Equer, Energie solaire photovoltaïque (volume 1: physique et technologie de la conversion photovoltaïque), 1ère édition, ELLIPES, Paris, 1993.

[21] Graham VA, Hollands KGT A method to generate synthetic hourly solar radiation globally, Solar Energy, 44 (6), pp. 333-341, 1990.

[22] Duffie JA, Beckman WA Solar Engineering of Thermal Processes 2nd edition, Wiley, New York, NY, 1991.

[23] **TradeKey.** *Air Cooling Gasoline Generator 0.65 kW – 7.5 kW* [en ligne]. S. l. : TradeKey, [s.d.]. Disponible sur : https://www.tradekey.com/product-free/Air-Cooling-Gasoline-Generator-0-65kw-7-5kw--1189782.html

[24] G.C. Seeling-Hochmuth, "A combined optimization concept for the design and operation strategy of hybrid-PV energy systems", Solar energy 61(2), pp. 77-87, 1997.

[25] O. Skarstein and K. Uhlen, "Design considerations with respect to long-term diesel saving in wind/diesel plants", Wind Engineering, Volume 13, pp. 72-87, 1989.

[26] I. Vechiu, " Modélisation analyse de l'intégration des énergies renouvelables dans un réseau autonome," 2005.

[27] Fatih O. Hocaogˇlu, O¨ mer N. Gerek, Mehmet Kurban "A novel hybrid (windphotovoltaic) system sizing procedure", Solar Energy 83 (2009), pp. 2019-2028.

[28] B. Ai, H. Yang, H. Shen, X. Liao, "Computer-aided design of PV/wind hybrid system", Renewable Energy 28 (2003), pp. 1491-1512.

[29] Market survey: "Inverters 2007", Photon International Avril 2007, p. 138.

[30] Elsevier / ScienceDirect. *"Figure 3 – Modèle ou schéma lié à un système photovoltaïque"*.https://ars.els-cdn.com/content/image/1-s2.0-S1546221822005902-CMC_30733-fig-3.jpg

[31] H. Patel and V. Agarwal, *“Maximum Power Point Tracking Scheme for PV Systems Operating Under Partially Shaded Conditions”*, IEEE Trans. Ind. Electron., 2008.

[32] Messenger, R. & Ventre, J., *Photovoltaic Systems Engineering*, CRC Press, 2010.

[33] Luque, A. & Hegedus, S., *Handbook of Photovoltaic Science and Engineering*, Wiley, 2011.

[34] NEC 2020, *National Electrical Code*, Section 690 – Solar Photovoltaic Systems.

[35] https://www.condor.dz/images/pdf/CatalogueProduitsSolairesPhotovoltaiques_ min.pdf. (accessed 21 December 2021).

[36] Les Dossiers de La Lettre du Solaire. Mai 2014 / Vol 5 N ◦ 05, Programmes PED, Publi´ ee par CYTHELIA sas. (accessed 21 December.2021).

[37] www.groupe-soprec.com

[38] www.energy.gov.dz

[39] www.gmi-groupe.com

[40] Dekkiche M, Tahri T, Denai M. Techno-economic comparative study of grid-connected PV/reformer/FC hybrid systems with distinct solar tracking systems. *Energy Convers Manag X* 2023;18:100360. https://doi.org/10.1016/j.ecmx.2023.100360.

[41] Al Garni HZ, Awasthi A, Ramli MAM. Optimal design and analysis of gridconnected photovoltaic under different tracking systems using HOMER. Energy Convers Manage 2018; 155:42–57. https://doi.org/10.1016/j. enconman.2017.10.090.